MID-AIR HAPTIC SENSATIONS PRODUCED BY ULTRASOUND ACTUATORS IN PATIENTS WITH CARPAL TUNNEL SYNDROME

by

Mehmet Akif Akdağ

B.S., in Electrical and Electronics Engineering, Boğaziçi University, 2019

Submitted to the Institute of Biomedical Engineering
in partial fulfillment of the requirements
for the degree of
Master of Science
in
Biomedical Engineering

Boğaziçi University
2023

ACKNOWLEDGMENTS

To Prof. Burak Güçlü, my supervisor, I am indebted for providing me with the direction and encouragement I needed to finish my thesis. His vast understanding, boundless energy, and unwavering support made this project achievable.

I wish to acknowledge the help and guidance provided by Kıvanç Menekşeoğlu, M.D., specialist in physical therapy and rehabilitation. With the help of his company, Kanguru Rehabilitation Tech., the Ultrahaptics STRATOS Explore device that was used in this thesis project was bought with the funding done by KOSGEB for the project title of "Neurological rehabilitation mediated by virtual reality and haptic systems". Also special thanks to Hatice Seğmen, M.D., specialist in neurology, who performed the electromyography and nerve conduction studies at Kanuni Sultan Süleyman Training and Research Hospital to aid our research.

I would like to express my gratitude to each member of Tactile Research Laboratory. I am honored to be a part of it. I thank to Deniz Kılınç Bülbül, Begüm Devlet Kılıçkap, and Sevgi Öztürk who have been the most encouraging and helpful lab mates during my whole thesis process. When I had a problem, they would patiently assist me figure it out. I appreciate everyone who took part in the experiments for their time and patience.

Also I am thankful to have Seda Tuğçe Ozantürk in my life who has been there for me in every aspect of my research since the day we met, and for that I am eternally grateful.

Finally, I would like to give my sincerest thanks to my family for their unwavering emotional and spiritual support as I worked on my thesis and throughout my life.

ACADEMIC ETHICS AND INTEGRITY STATEMENT

I, Mehmet Akif Akdağ, hereby certify that I am aware of the Academic Ethics and Integrity Policy issued by the Council of Higher Education (YÖK) and I fully acknowledge all the consequences due to its violation by plagiarism or any other way.

Name :

Signature:

Date:

ABSTRACT

MID-AIR HAPTIC SENSATIONS PRODUCED BY ULTRASOUND ACTUATORS IN PATIENTS WITH CARPAL TUNNEL SYNDROME

This thesis utilizes psychophysical experiments with mid-air haptic ultrasound actuators to assess carpal tunnel syndrome (CTS) patients' tactile sensation. 19 female and one male patients (age: 33-61) with unilateral CTS took part in the experiments. We used a two-alternative forced choice task experiments to measure detection thresholds around 250 Hz modulation frequency at the thenar eminence (TE) and at the index finger in affected and healthy hands. In addition, 15 female CTS patients participated in a virtual reality-assisted hand exercise game with haptic feedback. The system usability scale (SUS) and exercise performance scores were evaluated. There was no significant difference in the threshold values from the TE between the CTS hand (M=0.85 au, SD=0.15) and the healthy hand (M=0.87 au, SD=0.16). The thresholds measured from the index fingers of CTS affected hands were all higher than the maximum stimulus level that could be produced by the ultrasonic actuators. For the healthy hands of 17 patients, the detection thresholds were (M=0.90 au, SD=0.09), and the remaining 3 had threshold values above the maximum output of the device. For the exercise game results, there was a significant correlation ($\rho = 0.89$, $p < 0.001$) between the SUS (M=80.17%, SD=18.33) and performance scores (M=83.31%, SD=14.80). Since the CTS was at an early stage and there may be a branching (palmar cutaneous branch) of the nerve before entering the carpal tunnel, thresholds were found similar in both hands at the TE. Unfortunately, the limitations of the haptic device did not allow a comparison between index fingers. Moreover, this device and novel technology may be used for the follow-up of the rehabilitation and the treatment of the CTS. As such, the usability of the system is above the criterion value, and in the future it can be improved not to be affected from the performance in the exercise games.

Keywords: Touch, Psychophysics, Somatosensory System, Carpal Tunnel Syndrome, Pacinian Channel, Ultrasound Stimulus, Mid-Air Haptics.

ÖZET

KARPAL TÜNEL SENDROMLU HASTALARDA ULTRASONİK EYLEYİCİLER TARAFINDAN ÜRETİLEN HAVADA DOKUNMA DUYUSU

Bu tez, karpal tünel sendromlu (KTS) hastalarda, ultrasonik eyleyiciler tarafından üretilen havada dokunma duyusunu değerlendirmek için yapılan psikofiziksel deneyleri kapsamaktadır. Deneylere tek taraflı KTS'li 19 kadın ve bir erkek hasta (yaş: 33-61) katıldı. KTS'li ve sağlıklı ellerde tenar eminenste (TE) ve işaret parmağında 250 Hz modülasyon frekansı civarında algılama eşiklerini ölçmek için iki alternatifli zorlanmış seçim ödevi içeren deneyler yapıldı. Ayrıca, 15 kadın KTS'li hasta, dokunsal geri bildirim içeren sanal gerçeklik destekli bir el egzersizi oyununa katıldı. Sistem kullanılabilirlik ölçeği (SKÖ) ve egzersiz performans puanları ölçüldü. KTS'li el (M=0.85 au, SD=0.15) ve sağlıklı el (M=0.87 au, SD=0.16) arasında TE'de eşik değerleri açısından anlamlı bir fark bulunamadı. İşaret parmağından alınan ölçümlerde, KTS'li ellerin tamamında ve sağlıklı ellerin 3'ünde eşik değeri cihazın üretebildiği maksimum uyaran seviyesinden daha yüksek bir değer olarak tanımlandı. Sağlıklı ellerde kalan 17 hastanın eşik değeri (M=0,90 au, SD=0,09) kaydedildi. El egzersizi oyunu sonuçları için SKÖ (M=%80.17, SD=18.33) ve performans puanları (M=%83.31, SD= 14.80) arasında istatistiksel olarak anlamlı bir korelasyon ($\rho = 0.89$, $p < 0.001$) bulunmuştur. KTS'nin erken evrede olması ve TE bölgesine giden sinirde karpal tünele girmeden önce bir dallanma olabileceği için (palmar kutanöz dalı) TE'de eşik değerleri her iki elde de benzer çıkmıştır. Ancak, ultrasonik cihazın kısıtlaması sebebiyle işaret parmakları arasında tam bir karşılaştırma yapılamamıştır. Öte yandan, bu cihaz ve beraberinde getirdiği teknoloji, KTS'nin rehabilitasyonunda ve tedavisinin takibinde kullanılabilir. SKÖ literatürde belirtilen kriterin üzerinde olduğu için sunulan egzersiz oyunu, ilerde kullabilirliğin performanstan etkilenmeyeceği bir şekilde geliştirilebilir.

Anahtar Sözcükler: Dokunma, Psikofizik, Somatosensoriyel Sistem, Karpal Tünel Sendromu, Pacini Kanalı, Ultrasonik Eyleyici, Havada Oluşan Dokunma Duyusu.

TABLE OF CONTENTS

LIST OF FIGURES

LIST OF TABLES

LIST OF SYMBOLS

au	arbitrary unit
m/s	Meter per second
$^\circ$	Degrees
p	P value
n	Number of subjects
$\bar{x}$	Mean of the sample group
s	Standard deviation of the sample group
ρ	Pearson correlation coefficient
p	Probability of success

LIST OF ABBREVIATIONS

CTS	Carpal tunnel syndrome
VR	Virtual reality
AR	Augmented reality
3D	Three dimensional
AM	Amplitude modulation
STM	Spatio-temporal modulation
LED	Light emitting diode
USB	Universal serial bus
MRI	Magnetic resonance imaging
NSAIDs	Non-steroidal anti-inflammatory drugs
SA	Slowly adapting
RA	Rapidly adapting
SA1	Slowly adapting type 1 afferent
SA2	Slowly adapting type 2 afferent
RA1	Rapidly adapting type 1 afferent
RA2	Rapidly adapting type 2 afferent
S1	Primary somatosensory cortex
S2	Secondary somatosensory cortex
NCS	Nerve conduction study
ENMG	Electroneuromyograph
CMAP	Compound muscle action potential
SNAP	Sensory nerve action potential
EMG	Electromyography
RMSE	Root mean square error
SUS	System usability scale
CSAd	Cross-sectional area distal
CSAp	Cross-sectional area proximal
TE	Thenar Eminence

API	Application Programming Interface
DCN	Dorsal column nuclei

1. INTRODUCTION

1.1 Motivation

Carpal tunnel syndrome (CTS) is the most common compressive neuropathy in clinical practice, which is a medical condition that is caused by the compression of the median nerve [1, 2]. The median nerve is responsible for providing sensory and motor function to the thumb, index, middle, and half of the ring finger [3]. The general symptoms are numbness and pain in those regions; however, in some cases, the pain may extend to the arm.

Approximately, 3% of the population is affected by CTS, and CTS mostly begins in adulthood and affects mostly women [4, 5]. CTS can be caused by motions or activities requiring a lot of repetition and force [6]. Additionally, certain medical conditions, such as diabetes or arthritis also increase the risk of CTS [7]. Treatment options include wrist splints, medication, and, in severe cases, surgery, which may be necessary [8, 9].

Additionally, CTS can have a significant impact on a person's physical residual functional capacity. People with the disorder find it challenging to do repetitive chores on a daily basis. For activities of daily living, such as brushing teeth, buttoning clothes, and opening jars, people with this disease may require assistance from others due to the loss of fine motor skills and hand dexterity.

Because the symptoms typically appear gradually, it is also possible that those who are experiencing the disorder's early stages are unaware of their condition. It is important for individuals to be aware of the early signs of this disease and seek medical attention if they notice any changes in their fine motor skills. Notably, sensory fibers are more sensitive to compression than motor fibers, and the disorder is likely to first affect sensory fibers [10]. Early diagnosis and treatment is crucial because with the

help of therapies and exercises, patients can decelerate the progression of the CTS, thus can delay the carpal tunnel surgery.

Patients with this disorder should do regular hand exercises to improve their symptoms and avoid carpal tunnel surgery. It is also important for patients to maintain a healthy lifestyle and avoid activities that may worsen their symptoms. In some cases, medications may be prescribed to manage the pain and inflammation associated with the disorder [8].

New diagnostic techniques that are accessible outside the hospital may make it easier to identify CTS in its early stages. Also, with the help of the advancing virtual reality environment, those patients can better motivate themselves to exercise more and avoid carpal tunnel surgery, which will eventually reduce the impact of the disease on society.

1.2 Hypothesis

The primary objective of this study was to look at the mid-air haptic sensations produced by ultrasound actuators in patients with CTS by using the Ultrahaptics STRATOS Explore device which is given in Figure 2.1. The second objective was to test whether the ultrasound mid-air haptic technology can be used as a preliminary diagnosis method for CTS or not. Finally, the third objective was to test whether infrared imaging technology and haptic feedback by ultrasound can be used as a novel exercise method to improve the overall experience of the patients during exercise with the help of hand tracking software and virtual reality implementations.

According to the studies in the literature, nerve conduction studies (NCS) and medical ultrasound imaging are proven techniques for the diagnosis of CTS. However, these methods are not accessible outside of a medical institution, while the Ultrahaptics STRATOS Explore device can be accessed from anywhere. In this thesis, the Ultrahaptics STRATOS Explore device was used for mid-air haptic sensation generation

and for real time hand tracking.

For this thesis research project, I hypothesized that this novel mid-air ultrasound haptic technology can be used as an alternative diagnosis method for CTS after investigating its sensations in patients with CTS, and also that the overall rehabilitation and treatment for CTS can be improved with the help of this technology.

1.3 Outline

In the first chapter, the motivation and hypotheses of the study are presented. In chapter 2, a brief background on ultrasound mid-air haptics technology, leap motion hand tracking technology, CTS, the somatosensory system, electromyography, and nerve conduction studies is given. In the third chapter, the methodology of this study is explained. The results are presented in chapter 4. In the last chapter, the literature review, the general conclusion, limitations, and future work possibilities are discussed.

2. BACKGROUND

2.1 Ultrasound Mid-Air Haptics Technology

Ultrasound mid-air haptics is a novel technology that takes advantage of contactless haptic sensation. It creates the sensation of touch by vibrating the air and superficial skin tissues. Most other haptic devices require the user to wear equipment, which may disrupt feelings and sensations, whereas contactless haptic devices do not need direct physical contact, which is expected to improve user engagement in a scenario where the user is expected to interact with digital content [11].

Figure 2.1 Ultrahaptics STRATOS Explore device that has 16x16 array of transducers that are transmitting 40 kHz ultrasound waves and the Leap Motion Controller device (left side) [12].

Ultrasound haptic feedback mechanisms are expected to improve human computer interaction, and because of that, they have attracted significant attention from the haptics literature [13]. This technology has many promising application areas, such as automotive user interfaces, VR (virtual reality), and AR (augmented reality) [14, 15]. Martinez et al. suggested several mid-air haptic algorithms for rendering 3D shapes, which are expected to improve tactile sensation [16]. Georgiou et al. have presented the world's first mid-air haptic rhythm game, and due to its dynamic and contactless environment [15]. Also, Martinez et al. designed a game where the user is an apprentice wizard learning the lightning spell [17]. By changing the movement pattern of an ultrasonic focus point, they have shown how a varied set of sensations can

be evoked. Hwang et al. designed AirPiano, which is a virtual reality piano playing experience that takes advantage of mid-air ultrasound haptic feedback [18]. Freeman et al. designed HaptiGlow, which uses mid-air ultrasound haptic feedback to help users position their hands better in the air, which is expected to improve many mid-air digital applications [19].

In this technology, the sense of touch is created by ultrasound waves that are travelling by vibrating the air. Several actuators are synchronizing to create high amplitude areas at the desired location with the help of phase shifting. Those high amplitude focus areas can be created and moved with ease. High sample rates and the speed of sound help provide an excellent level of temporal accuracy as well [20].

Ultrasound is a term for sound waves with a frequency higher than what people can hear, which is around 20 kHz but varies between individuals. In Figure 2.2, a single transducer is not capable of creating the required pressure on the human skin, so phased array focusing techniques are used to generate a focal point at the desired location. The attainable amplitude is greatly increased by focusing many actuators to the desired focal point. Each wave's phase is shifted so that it reaches the desired location simultaneously, causing pressure to build up in the focal point. We use the term "focal point", but it is not actually a point. It is an ellipsoid that can get elongated or distorted based on where the focal point is on the device [20]. The compression areas in the longitudinal sound wave create the high amplitude peak points, and the mid-air haptic device creates its focal points by combining all high energy compression areas that are created by 256 actuators on the array.

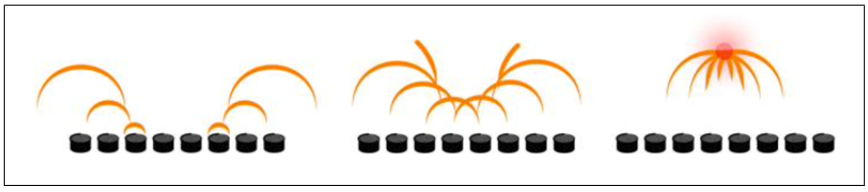

Figure 2.2 Demonstration of how a focal point is created in mid-air. From left to right each image represents the consecutive stages [20].

The Ultrahaptics STRATOS Explore Device uses a 40 kHz carrier signal. An

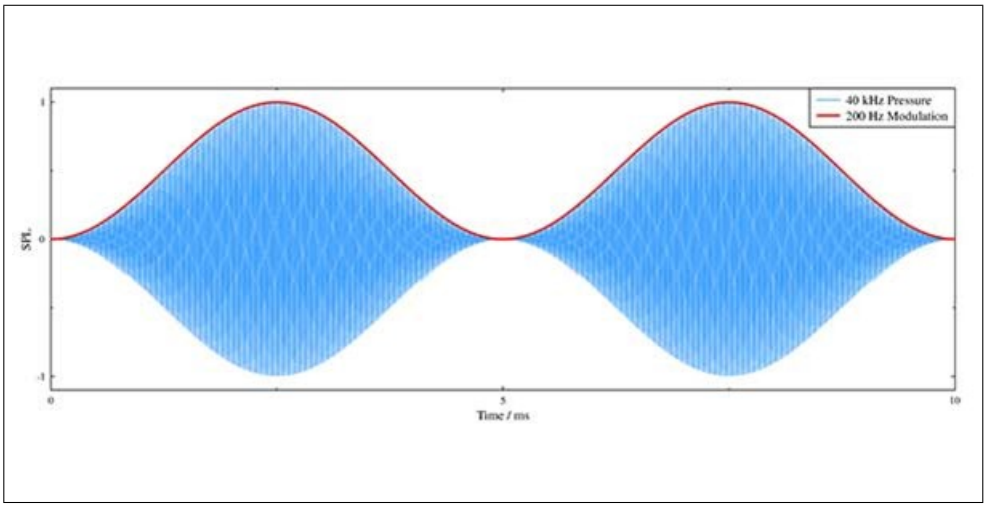

Figure 2.3 An example signal: 40 kHz carrier signal enveloped by the 200 Hz modulation signal.

example signal that is created by this device can be seen in Figure 2.3 the 40 kHz ultrasonic transducers are common in medical applications such as diagnostic testing and surgical devices, as well as cleaning devices like vehicle detection for car washes, manufacturing for an automated process, robotic sensing, presence detection, people detection for counting.

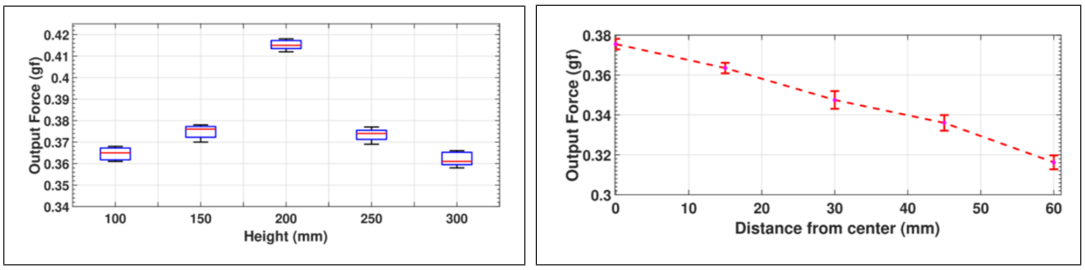

Figure 2.4 Effect of vertical distance on the output force at 240 Hz (left). Effect of horizontal distance on the output force (right) [21].

Raza et al. measured the output pressure of the Ultrahaptics STRATOS Explore device in their studies to figure out how vertical and horizontal distance affect the strength of the signal [21]. According to their study, the ideal distance is 20 cm away from the haptic device, and the output force is decreasing as we move horizontally away from the center of the array, as shown in Figure 2.4. Raza et al. also worked on the absolute threshold values at several modulation frequencies, and they showed that the absolute threshold versus frequency plot has U-shape characteristics, which

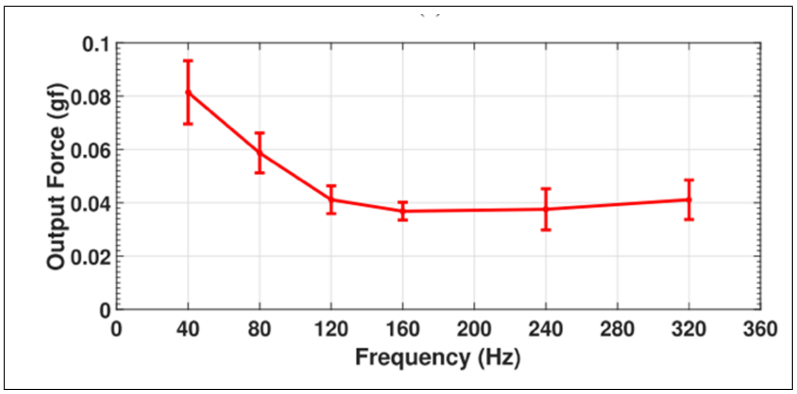

Figure 2.5 Threshold values on several frequencies at 250 mm height [21].

means the threshold has its lowest value around 160-250 Hz, and for other values it increases [21]. The frequencies and their corresponding absolute threshold values are presented in Figure 2.5. The same result was also approved by a study done by Rakkolainen et al. [22]. Carter et al. through psychophysical research showed that feedback points with distinct tactile qualities may be detected despite the very close proximity of the points [23]. They also demonstrated that, after receiving proper training, participants easily discriminate mid-air ultrasound stimulus having different frequencies [23]. The increase in percentage accuracy after each training session can be seen in Figure 2.6. A research about the tactile sensation generated by airborne ultrasound was done by Iwamoto et al., they reported that the participants clearly felt the stimulus when it is modulated by burst waves with a frequency ranging between 20-250 Hz [13]. According to their study, the total output force is measured as 0.8 gf when the vertical distance was 25 mm above the array [13]. Also, by using a condenser microphone, they measured the spatial resolution as 20 mm[13]. Frier et al. worked on sampling strategies to show that whether they affect the circular pattern perception or not [24]. They found that the effect of update rate on the perceived strength is much more visible for slow rates around 10 Hz or less; however, for higher update rates does not affect pattern perception [24]. Also in their study, optimal sampling rates and threshold sampling rates were measured for different pattern draw frequencies[24]. Hajas et al. also compared static and dynamic rendering performance of 2D shapes to discuss their effects on the users [25]. According to their study, shapes are recognized more frequently with higher confidence levels when dynamic rendering techniques are

used [25]. Dynamic rendering techniques use spatio-temporal modulation (STM) while static rendering techniques use amplitude modulation (AM), which is shown in Figure 2.7.

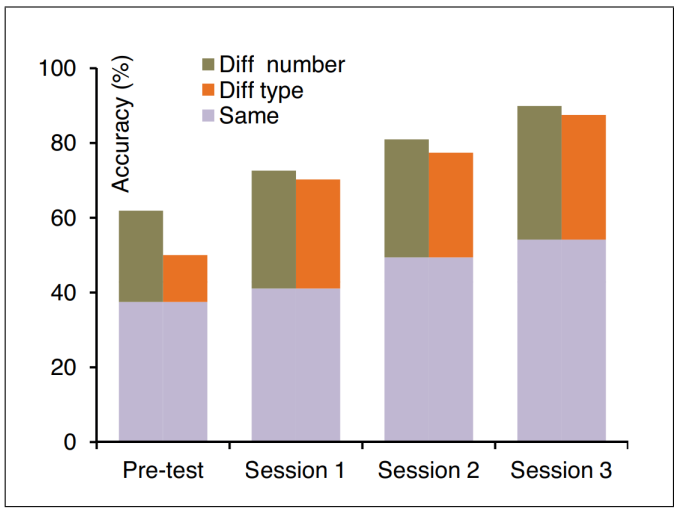

Figure 2.6 Accuracy rates are given for two stimulus having the same frequency value (same), or there are two different stimuli (Diff number), or there are two different stimulus in terms of frequency type (Diff type) [23].

The focal point size depends on the frequency of the carrier signal. A higher frequency yields a smaller diameter for the focal point because it has a smaller wavelength. For the Ultrahaptics STRATOS Explore device, the carrier frequency is 40 kHz. Combining that information with the speed of sound at room temperature, which is around 346 m/s, we have a wavelength of 8.6 mm. Each control point is about 8.6 mm in diameter [26].

The Ultrahaptics API supports amplitude modulation (AM) and spatio-temporal modulation (STM), as represented in Figure 2.7. Amplitude modulation is limited to discrete focal points where we have the freedom to change their intensity, while spatio-temporal modulation uses one single focal point and can move back and forth in a certain line or curve.

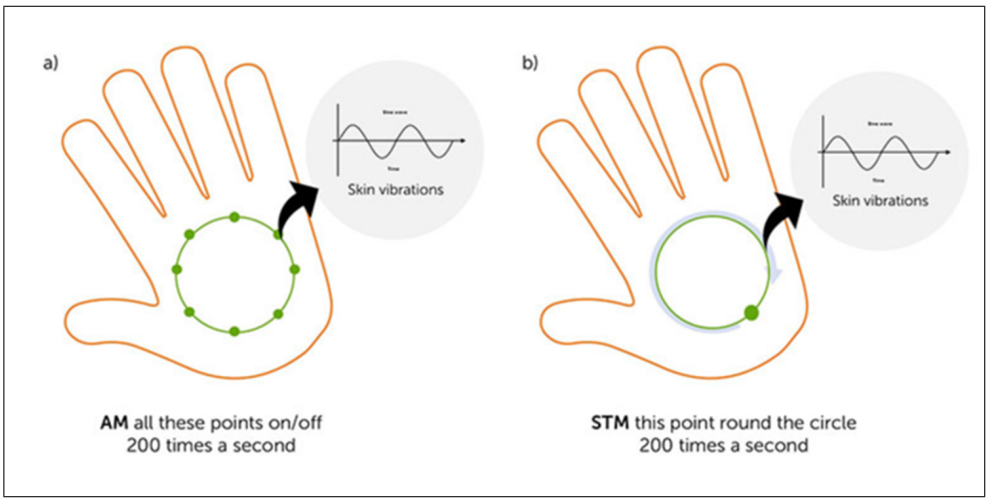

Figure 2.7 Generation of (a) AM and (b) STM signals [26].

2.2 Leap Motion Hand Tracking Technology

The Leap Motion Controller, comes with the Ultrahaptics Stratos Explore device, is an optical hand tracking device, which can be seen in Figure 2.8. The main components of the device are two cameras and a few infrared LEDs that emit infrared light at 850 nanometers, which is invisible to the human eye [27]. Due to the synchronization of the cameras and LEDs, power consumption is reduced while intensity is increased. A wide interaction zone where a user's hands can be detected is created using wide angle lenses. For instance, the Leap Motion Controller's 140°x120° field of view and typical interaction zone range from 10 cm to 60 cm or more [27]. However, beyond a certain distance, it becomes challenging to track a user's hand position in 3D due to the range being constrained by LED light propagation through space. Before streaming the sensor data via USB to the software, the hand tracking device's USB controller reads the sensor data and makes any necessary adjustments.

Grayscale stereo images of the near-infrared light spectrum that were taken by the left and right cameras are used to display the data, as shown in Figure 2.9. The device's LEDs will illuminate objects, but daylight, halogens, and incandescent light sources will also be visible. Additionally, it's important to keep in mind that some objects, such as cotton shirts, may appear white even though they are dark in the

visible spectrum.

Figure 2.8 Leap Motion Controller [27].

Figure 2.9 Grayscale stereo images [27].

Following the transmission of the image data to a computer, complex mathematical operations are needed. The images are then examined to reconstruct a 3D model of what the device perceives after being corrected to account for background objects like heads and environmental lighting [27]. The hand tracking algorithms examine the 3D ball and stick model data to determine the locations of hidden objects, while the tracking layer compares the data to identify tracking information like fingers. The 3D ball and stick model and the exercise scene is shown in Figure 2.10. Filtering techniques are used to make sure the data is consistent over time and flows easily [27].

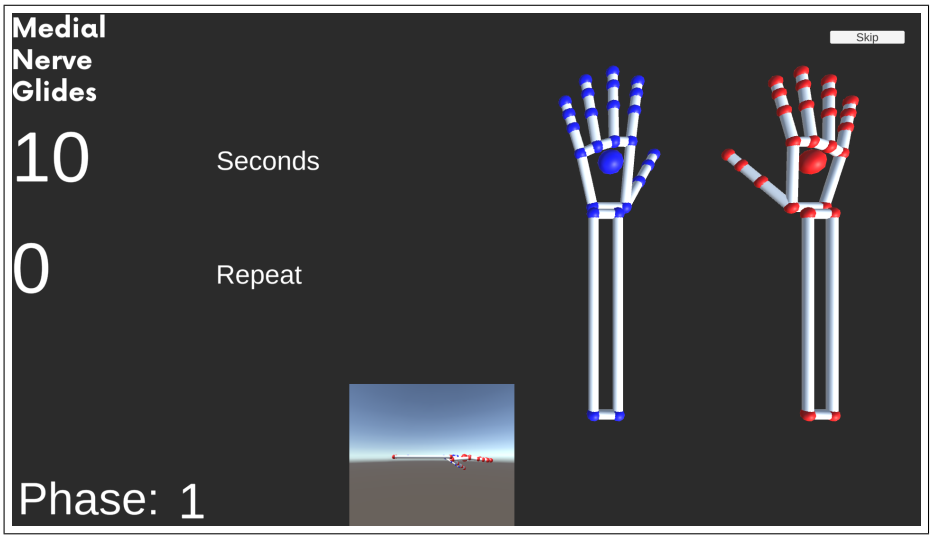

Figure 2.10 3D ball and stick model, and the exercise scene.

2.3 Carpal Tunnel Syndrome

CTS occurs due to the compression of the median nerve when it travels through the carpal tunnel [1, 2]. The median nerve and the branches of the median nerve can be seen in Figure 2.11 [28]. The index, middle, and radial side of the ring fingers, as well as the palm side of the thumb, are all sensed by the median nerve. Additionally, the median nerve controls the muscles of the anterior forearm and some muscles in the thenar eminence of the hand. The anterior forearm muscles are responsible for wrist flexion, finger flexion, and thumb opposition. The thenar eminence is the fleshy area at the base of the thumb, and the median nerve controls the muscles that allow for opposition and abduction of the thumb, as well as some of the muscles responsible for flexion of the fingers.

The symptoms often develop over time and generally peaks at nights[30]. Typically, the dominant hand is the first to be afflicted [31]. People may experience tingling throughout the day as their symptoms increase, particularly while engaging in specific activities like chatting on the phone, reading a book or newspaper, or driving. It could be challenging to handle tiny things or carry out other manual chores if your hands are weak. In conditions that are chronic or that go untreated, the muscles that are located around the base of the thumb may atrophy over time [8]. Some people with extremely

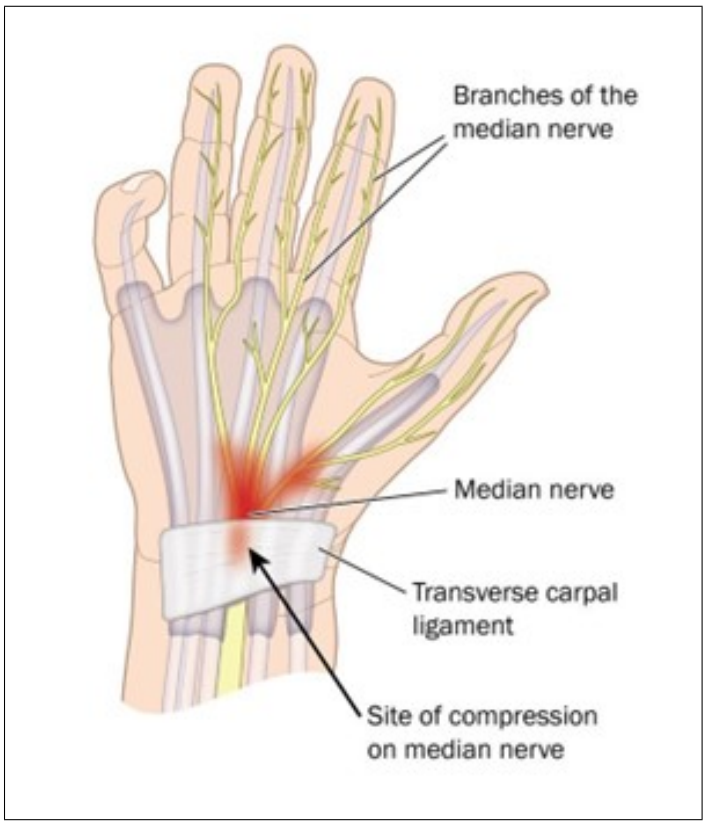

Figure 2.11 CTS affected median nerve and its branches [29].

severe CTS are unable to differentiate between heat and cold by touch, which may result in accidental finger burns.

Instead of being caused by a problem with the nerve itself, CTS can be the consequence of a number of variables working together to increase the amount of pressure that is placed on the tendons and the median nerve that are enclosed within the carpal tunnel.

Contributing factors can be listed as:

- Repetitive motions: CTS can be caused by repetitive stress on the median nerve from activities including typing, computer mouse use, playing an instrument, or working on an assembly line.
- Injury or trauma: Fractures, sprains, dislocations, or any other injury to the

wrist or hand can cause swelling, which can compress the median nerve and lead to CTS [32].

- Arthritis: Arthritis, especially rheumatoid arthritis, can cause inflammation and swelling of the wrist joint, compressing the median nerve and causing CTS.
- Pregnancy: During pregnancy, the body retains more fluid, which can increase the pressure on the median nerve and lead to CTS [3, 33].
- Hormonal changes: Hormonal imbalances, such as thyroid disorders, menopause, or diabetes, can affect the health of the nerves and lead to CTS.
- Obesity: Excess weight can increase the pressure on the wrist and hand, leading to CTS [33].
- Genetics: In some cases, CTS can be inherited or run in families, suggesting a genetic component to the condition [28].

The median nerve may already be under strain or already be damaged as a result of workplace circumstances. Although the risk of CTS is not specific to any one profession or sector, it may be more common among workers [6]. In order to avoid permanent damage, early diagnosis and treatment are crucial. Generally, a physical examination is necessary to show whether CTS occurs due to an underlying health issue or due to daily activities. A medical professional may rule out the possibility of other conditions that are similar to CTS. The sensitivity of each finger should be assessed because in CTS, little finger's sensitivity can be used as comparator with other fingers to identify the CTS.

In the literature there are several tests that are used for CTS. The Tinel test can be used, where an expert kindly taps or presses the patient's wrist, if there is any kind of numbness or pain during that procedure, it indicates CTS [3]. The next one is the Phalen test, also known as wrist-flexion test. In this test CTS patient maintains a wrist-flexion pose in order to reveal CTS symptoms [34]. Also, if needed, doctors may request any kind of hand pose that can reveal the symptoms of CTS.

Electrodiagnostic testing might be helpful in the diagnosis of CTS [35]. The nerve conduction study (NCS) is one example, where electrodes are used to generate electrical signals on human body and the transmission speed is measured to assess the compression of the median nerve [36]. Electromyography (EMG) is another example, but it differs from the NCS because in EMG needles are inserted into muscle to monitor the electrical activity [36]. Another method is ultrasound imaging, where the median nerve might appear abnormally large [37]. MR imaging clearly shows median and ulnar nerves and their intraneural fascicular structure in the carpal tunnel [38, 39, 40].

CTS treatment methods can be divided into two categories: non-surgical treatments and surgical treatments.

1. Non-surgical Treatments:

    - Splinting: Typically, a nighttime splint is used as the first therapy [9].
    - Avoiding activities throughout the day that can exacerbate symptoms. Some people who experience mild pain may want to stop working often to rest their hands. Applying cold packs might be beneficial if the wrist is swollen, red, and heated.
    - Over-the-counter drugs: In some situations, a number of drugs may reduce the swelling and discomfort brought on by CTS. Aspirin, ibuprofen, and other over-the-counter pain medicines are examples of nonsteroidal anti-inflammatory drugs (NSAIDs), but they haven't been shown to be effective in treating CTS [41].
    - Prescription medicines: For people with moderate symptoms, corticosteroids or the medication lidocaine can be taken [42, 43].
    - Alternative therapies: Chiropractic and acupuncture treatments has positive effects on some people, but it is yet unknown if they are helpful. However, yoga is an exception in this category, since it has been shown to lessen discomfort and increase grip strength in people with CTS [3, 44].

2. Surgery:

One of the most popular surgical treatments is carpal tunnel release. To reduce pressure on the median nerve, a common surgical procedure involves cutting a ligament around the wrist. Surgery often involves mild sedation and is performed under local or regional anesthesia [45, 46, 47], so an overnight hospital stay is not necessary. Many patients need to have both hands operated on.

Open release surgery is the conventional method of treating CTS. During this procedure, an incision of two inches is made in the patient's wrist, and the carpal ligament is then severed in order to enlarge the carpal tunnel. Unless there are exceptional medical problems, the surgery is often performed on an outpatient basis while under local anaesthetic.

Compared to open release surgery, endoscopic surgery may result in a slightly faster functional recovery and less postoperative discomfort, but it may also bear a higher risk of complications and necessitate additional surgery [47]. The physician makes one or two microscopic incisions in the wrist and palm, inserts a camera connected to a tube, views the nerve, ligament, and tendons on a monitor, and then uses a small scalpel to sever the carpal ligament, the connective tissue between the joints. After surgery, ligaments often regenerate, creating more space than before. Despite the possibility of immediate symptom relief following surgery, full rehabilitation from carpal tunnel surgery could take months. Some individuals may experience infections, nerve injury, rigidity, and pain near the scar as a side effect. Typically, grip strength declines, but eventually improves. After undergoing surgery, the majority of people must adjust their work schedule for a few weeks, and some may need to shift jobs once they have fully recovered.

To prevent CTS, workers may engage in on-the-job fitness, stretch routines, take regular breaks from work, and adopt good posture and wrist positioning. Gloves without fingers may keep hands warm and flexible. It is possible to adapt worksta-

tions, tools, tool handles, and jobs to allow employees to keep their wrists in a natural posture while doing their duties. Worker rotation is an option. Employers may create programs in ergonomics, which is the practice of adjusting working circumstances and job requirements to employees' skills.

2.4 The Somatosensory System

The somatosensory system is a complex network of nerves, receptors, and brain regions that work together to process and interpret sensory information from the body [48]. This system is responsible for our ability to perceive touch, pressure, pain, temperature, and other physical sensations [48].

The somatosensory system is composed of three main parts: the sensory receptors in the skin, muscles, and joints, the nerves that transmit sensory information to the spinal cord and brain, and the brain regions that process and interpret the sensory information.

There are several types of sensory receptors in the skin, including mechanoreceptors, which respond to pressure, vibration, and stretch; thermoreceptors, which respond to changes in temperature; and nociceptors, which detect potentially harmful stimuli like heat, cold, or injury.

The sensory information travels through the peripheral nerves to the spinal cord and then to the brainstem and thalamus. From there on, it is processed and interpreted in the somatosensory cortex, a region of the brain responsible for mapping different body parts and processing different types of sensory information.

2.4.1 Sensory Receptors

The glabrous skin has four different kinds of mechanoreceptors that are in charge of the touch sensation [49]. Meissner corpuscles, Merkel cells, Pacinian corpuscles, and Ruffini endings are the four different types of mechanoreceptors found in the glabrous skin of the hands and feet, as shown in Figure 2.12 [49]. A decrease in sensitivity to a stimuli that occurs as a result of prolonged exposure to that stimulus is an example of sensory adaptation [50]. Because they continue to activate in response to consistent pressure on the skin, two of these receptors are categorized as slowly adapting (SA). The other two receptors, known as rapidly adapting (RA) receptors, react to skin motion but not to constant pressure. Figure 2.12 demonstrates that the RA1 mechanoreceptors produce a response whenever there is a change in the stimulus level, especially in the ramp section. On the other hand, the RA2 mechanoreceptors only respond to the sharp turns of the stimulus signal, which corresponds to the corners of the stimulus. In contrast, the SA1 mechanoreceptors respond to the entire stimulus, including the ramp and hold portions with an irregular firing pattern. Similarly, SA2 also reacts to the entire stimulus, although with a regular firing pattern [51]. Looking at the receptive field sizes in Figure 2.12, we see that RA2 and SA2 have larger receptive fields compared to RA1 and SA1.

Slowly adapting type 1 (SA1) fibers innervate the Merkel cells [52]. Their sensitivity to edges, corners, and points makes them excellent indicators of the amount of pressure being applied to the skin [52]. Despite having receptive field sizes of 2-3 mm, individual SA1 afferents can perceive spatial detail of 0.5 mm [53]. They ability to discriminate between textures are crucial for reading Braille.

Slowly adapting type 2 (SA2) fibers innervate the Ruffini endings [54]. These receptors are more sensitive to the form of big items held in the hand because they react more strongly to stretching than to skin indentation [54]. Additionally, they indicate finger and other joint motions that strain the skin above.

Rapidly adapting type 1 (RA1) fibers innervate Meissner corpuscles that rapidly

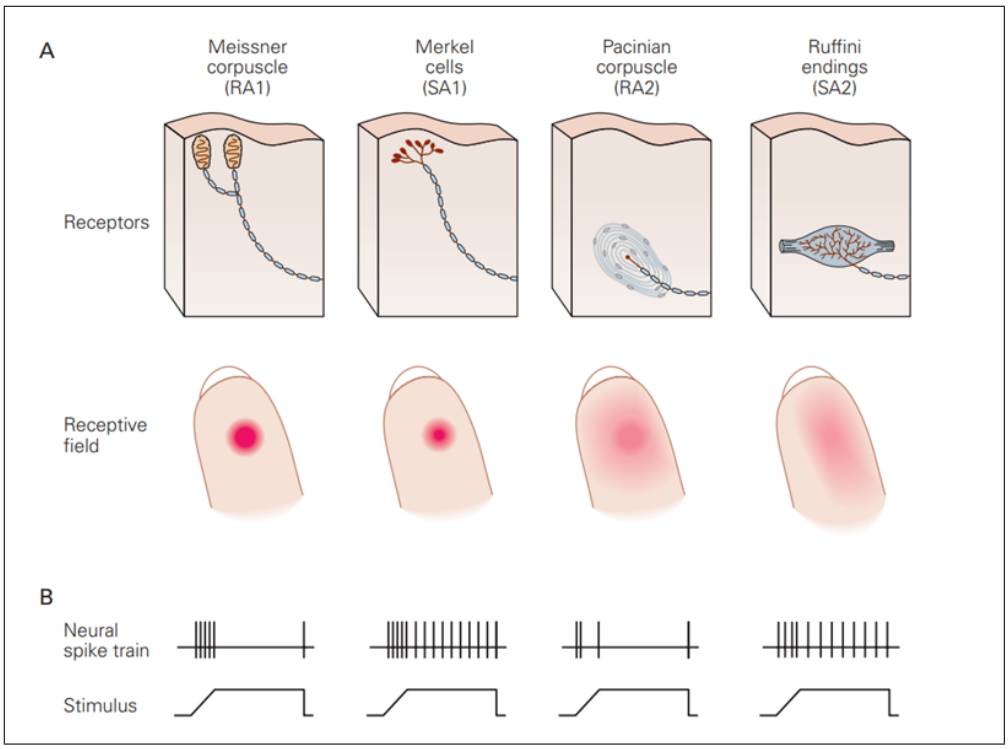

Figure 2.12 (A) 4 type of mechanoreceptors (top) and their corresponding receptive fields (bottom) (B) Different neural responses of 4 type of mechanoreceptors to the same stimulus [49].

adapts to the changes in texture [55]. These sensors pick up on the hand's first touch with an item, the object slipping out of the hand while it's being held, the hand moving across rough surfaces, and low-frequency vibration [55]. The Meissner corpuscle is the only mechanoreceptor organ absent from the general hairy skin; the hair follicle afferents provide a similar role to that of the Meissner corpuscle [56].

Rapidly adapting type 2 (RA2) fibers innervate the Pacinian corpuscles. Pacinian corpuscles assess coarse touch and discriminate between hard and soft materials [57]. They respond quickly, particularly to vibrations about 200 Hz, with action potentials [58]. The deep location of Pacinian corpuscles and its fibers' extraordinary sensitivity make them almost incapable of spatial resolution. They heavily filter the low-frequency signals with fuid-filled lamellae to prevent Pacinian corpuscle overstimulation. They have extensive receptor fields and are the most vibration-sensitive organisms [58]. Pacinian corpuscles only respond to abrupt stimuli; therefore, pressures like the constant compression of clothing are rapidly disregarded. They have also been linked

to the detection of where touch sensations are felt on handheld instruments.

Overall, the different types of mechanoreceptors work together to allow us to feel a wide range of tactile sensations, including texture, pressure, vibration, and movement. Their structure and function are optimized for specific types of stimuli, allowing us to sense and interpret the world around us through our skin.

2.4.2 Sensory Pathway

The skin undergoes a mechanoelectric transduction in response to the mechanical stimulation of the mechanoreceptors, resulting in the generation of brain activity. Myelinated nerve fibers are responsible for the transmission of the action potential, while unmyelinated nerve terminals able to perform mechanoelectric transduction. Tactile mechanoreceptors are considered primary receptors, and this information is transported to the dorsal root ganglia. The dorsal column then sends the signal to the dorsal column nuclei (DCN) in the brainstem. The neurons of the thalamus, also known as second-order neurons of somatosensation, are responsible for the formation of the second synapse in the medial lemniscal system, which is shown in Figure 2.13.

The output is sent to the primary somatosensory cortex (S1) and the secondary somatosensory cortex (S2) which are both found in the parietal lobe [51]. Specific colums that serve as an anatomical structure that contain neurons in the somatosensory cortex get inputs from a particular region of receptor sheets in the body, and they react to the same receptors that are being stimulated. SA and RA fibers are the conduits via which adjoining columns receive information from neighboring fingers, which is shown in Figure 2.14.

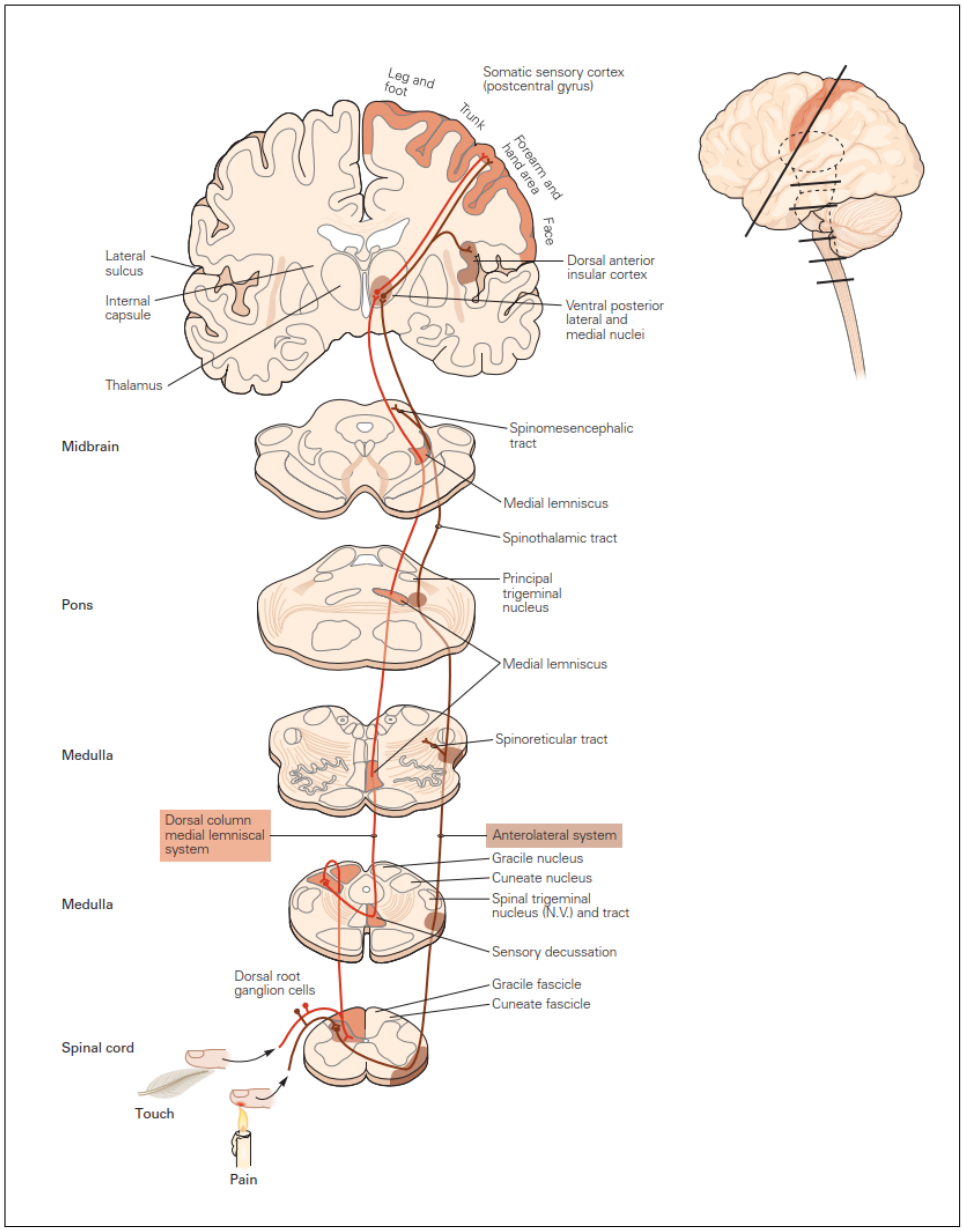

Figure 2.13 Somatosensory pathways that convey tactile information which originates from touch and pain [49].

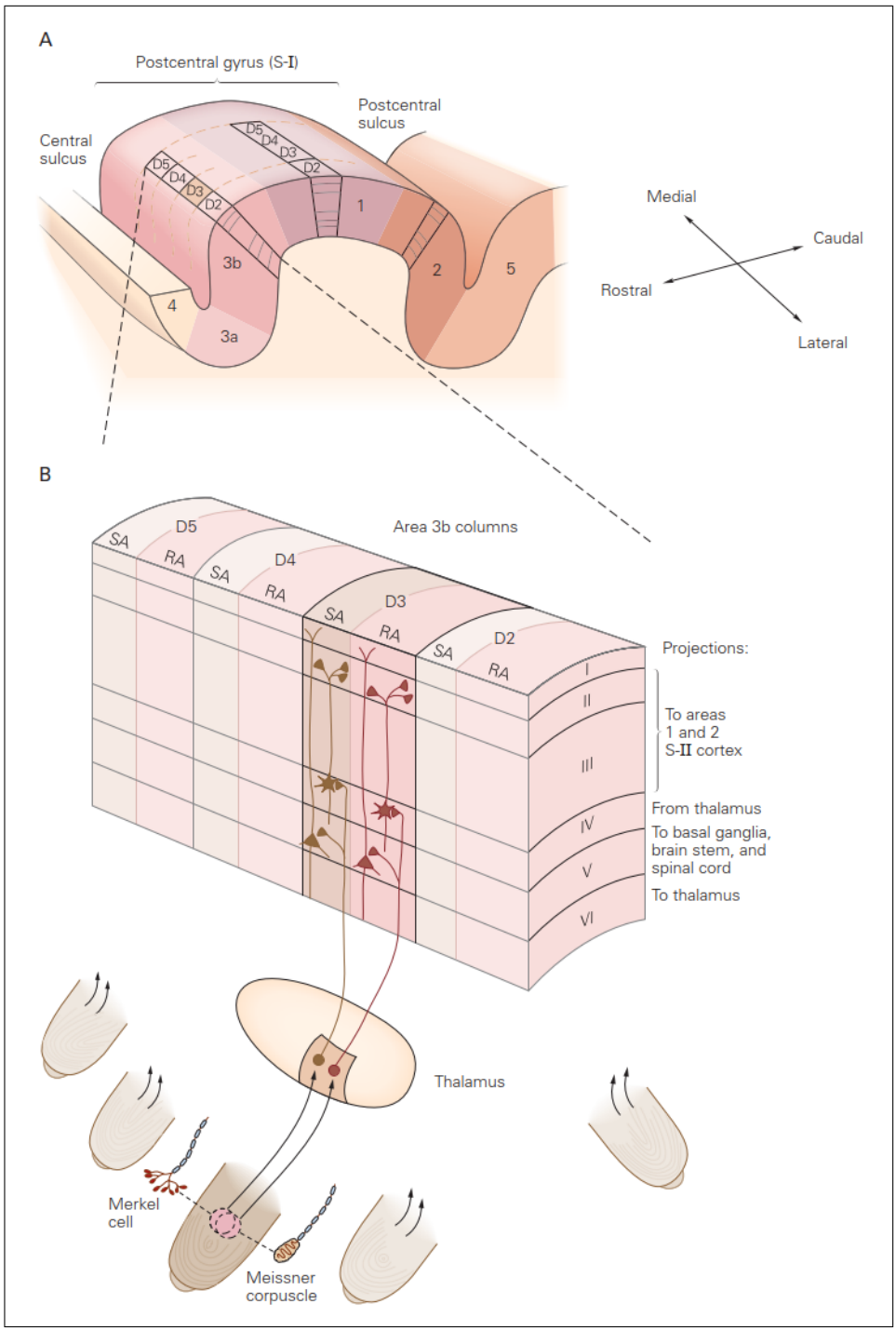

Figure 2.14 Organization of somatosensory cortex in columnlike fashion [49].

2.4.3 Four Channel Model that Mediates Tactile Perception

Psychophysical channels are important for investigating sensory systems, and their activity level determines the characteristics of stimuli. Verrillo discovered that detection thresholds at high frequencies have a U-shaped structure, while at low frequencies they do not vary with frequency [55, 59]. Additionally, the U-shaped part corresponds to P channel while the other flat parts corresponds to NP channel. Two techniques, selective adaptation and masking, were used to selectively isolate one channel. Selective adaptation raises one channel's threshold to calculate other channels' detection thresholds across a wide frequency range. Selective adaptation divided NP channels into two subtypes, NPI and NPII. Masking allowed for the existence of NPI and NPII channels, as well as the NPIII channel [60, 61]. Bolanowski's research identified four distinct categories of channels associated with specific fibers in glabrous epidermis [61]. Modifying stimulus properties, frequency, contactor size, masking techniques, and surface temperature yielded channel characteristics [62, 63, 64]. The NPI, NPII and NPIII channel characteristics with respect to their sensitive frequencies are shown in Figure 2.15.

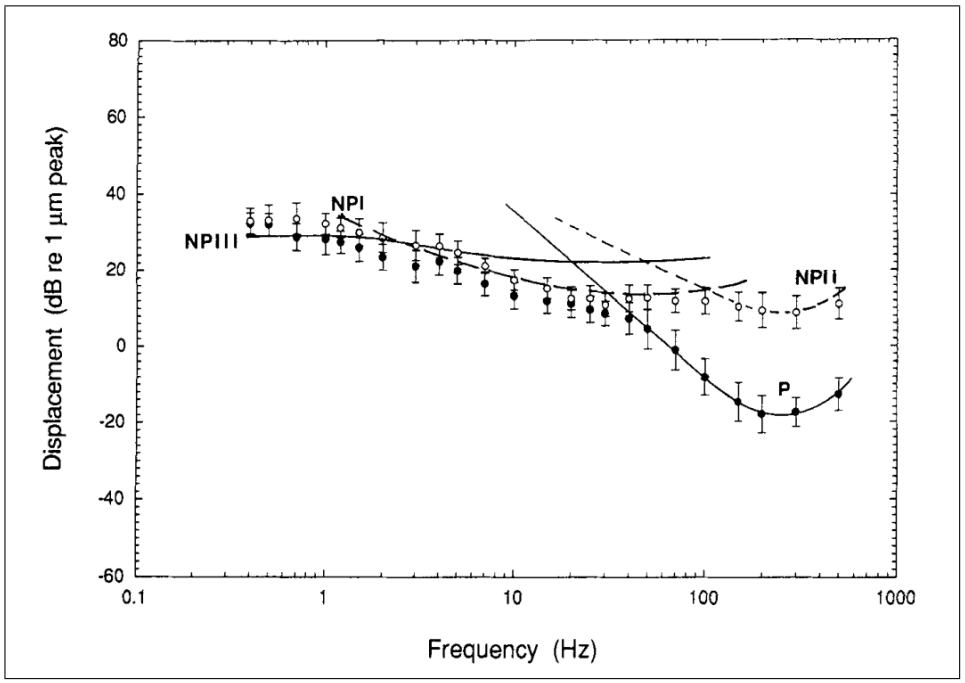

Figure 2.15 Four channel that mediate the tactile perception [65].

The Pacinian (P) channel is mediated by Pacinian corpuscles, which are predominantly sensitive to vibrational stimuli in the frequency range of 40-500 Hz. In the threshold-frequency curve, it displays a distinctive U-shape with the most sensitive region located close to 300 Hz [66]. Alterations in the temperature of the skin's surface have a significant impact on this channel [62]. In addition to this, Pacinian channels are capable of spatial summation, which implies that the detection threshold will drop as the contactor size increases. On the other hand, non-Pacinian channels are unable to perform spatial summation of the signal. In addition, Pacinian channels have the potential of temporal summation, which, when activated, causes a drop in detection threshold. This effect is triggered by an increase in the length of the stimulating event.

The non-Pacinian I (NPI) channel has a threshold response that is generally flat across vibratory frequencies, and it is less sensitive to variations in stimulus frequency than the P channel. The vibration frequencies that are considered to be within the normal working range of the NPI channel vary from 10 to 100 Hz. It does not exhibit either temporal or spatial summation, and it does not appear to be impacted by changes in temperature [62, 67]. The RA fibers, which are thought to innervate Meissner corpuscles, are probably the physiological analog of NPI. It is believed that these fibers innervate Meissner corpuscles.

The non-Pacinian II (NPII) channel is innervated by Ruffini endings. It operates in the vibratory frequency range that is close to the range of the P channel, which is approximately 15-400 Hz, but at a sensitivity that is considerably less. Only when the small contactor is utilized is the frequency-response curve of NPII determined. It is not capable of temporal and spatial summation like NPI channels [68].

The non-Pacinian III (NPIII) channel is mediated by Merkel's cell and seems to be functioning between 0.4 to 100 Hz and has an average sensitivity that is comparable to that of the NPI channel [61]. It is not capable of temporal and spatial summation. The size of the contractor does not affect the frequency-response curve.

2.4.4 Somatosensory Cortex

The processing of sensory data pertaining to touch, warmth, and pain from diverse regions of the body is carried out by the somatosensory cortex, a region of the brain. It is situated in the cerebral cortex's parietal lobe, with several sections correlating to various body parts.

The primary somatosensory cortex (S1) and the secondary somatosensory cortex (S2) are the two major regions of the somatosensory cortex, represented in Figure 2.16. Basic sensory data, such as the position and force of a touch or the temperature of an object, are processed by the primary somatosensory cortex [69]. It is divided into four sections that represent the face, upper extremities, trunk, and lower extremities of the body, respectively [70, 71].

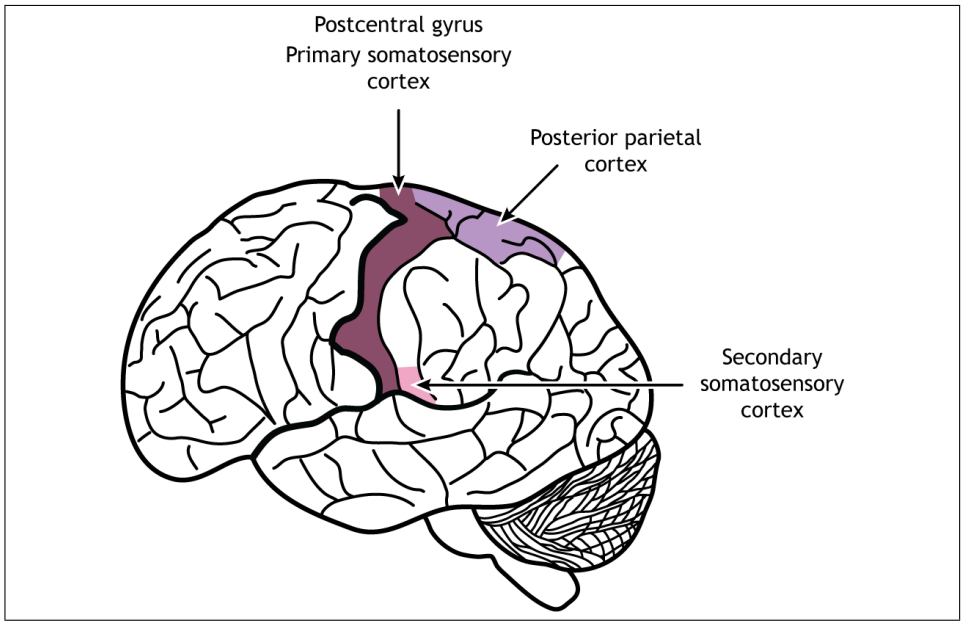

Figure 2.16 Primary and secondary somatosensory cortex [72].

Contrarily, processing more intricate sensory data like an object's texture and shape falls under the purview of the secondary somatosensory cortex. It is arranged into areas that correspond to various body parts and is situated next to the main somatosensory cortex [73, 74].

The somatosensory cortex gathers sensory data from all throughout the body's sensory receptors and transmits it along sensory neurons to the spinal cord and finally the brain. The somatosensory cortex then processes the data, enabling humans to recognize and make sense of various feelings. Sensory deficiencies, such as lack of feeling or modifications in how one perceives touch, warmth, or pain, can be brought on by damage to the somatosensory cortex. Damage in some situations can result in disorders like tactile agnosia, which prevents a person from recognizing items by touch, or astereognosis, which prevents a person from recognizing objects by touch and form. The somatosensory cortex performs both motor planning and execution in addition to processing sensory data. Input from the motor cortex is received, and it aids in the integration of sensory and motor information to enable coordinated movement.

Overall, somatosensory cortex function is critical for appropriate sensory perception and motor control, and it plays a significant role in how we perceive and understand the world around us.

2.5 Nerve Conduction Studies

An electrodiagnostic examination called a nerve conduction study (NCS) is performed to assess how well the peripheral nervous system is working [75, 76]. These tests assess the intensity and speed of electrical signals (compound action potentials) that pass through the body's muscles and nerves, revealing vital details about the condition and operation of these tissues [75].

2.5.1 Fundamentals of Nerve Conduction Studies

Studies of nerve transmission are based on electrophysiological concepts, which examine the electrical characteristics of biological tissues. The peripheral nervous system is made up of two different kinds of nerves: motor nerves, which carry signals from the brain to the muscles, and sensory nerves, which carry signals from the body to the

brain [77]. These nerves are made up of bundles of nerve fibers that are encased in insulating connective tissue and myelin sheaths.

Small surface electrodes are positioned on the skin above the nerves being evaluated during a nerve conduction study. One of the electrodes is then used to provide a modest electrical current to the nerve, while the other electrodes are used to record the electrical activity that takes place [76]. The test examines the amplitude, or the amount of electrical signal, and the latency, or the amount of time it takes for the electrical signal to travel from the stimulation site to the recording electrode.

In motor studies, the compound muscle action potential (CMAP) amplitude is measured as the difference between the negative peak voltage value and the base voltage value where the distal latency is measured from the first stimulation to the first voltage deviation which can be seen in Figure 2.17 [78]. In contrast, the sensory nerve action potential (SNAP) amplitude is measured from peak to peak voltage, and the distal latency is measured up to the negative peak of acquired waveform [78]. The distance between recording and stimulation sites can be divided by delay to get the velocity of the nerve conduction. The measurement that results is known as the conduction velocity, and it captures how quickly the nerve signal moves through the nerve [75, 76]. The quantity of nerve fibers that are stimulated by the electrical stimulation is reflected in the electrical signal's amplitude [75]. The CMAP recording from thenar eminence is shown in Figure 2.17. The SNAP recording and orthodromic stimulation sites are presented in Figure 2.18.

2.5.2 Procedures for Nerve Conduction Studies

Nerve conduction investigations are typically carried out between 30 and 60 minutes by a neurologist or an electrodiagnostic technician. The patient is requested to take off any clothes or jewelry that could get in the way of the electrode insertion before the test. To establish proper contact between the electrodes and the skin, the skin is then cleansed using an alcohol swab.

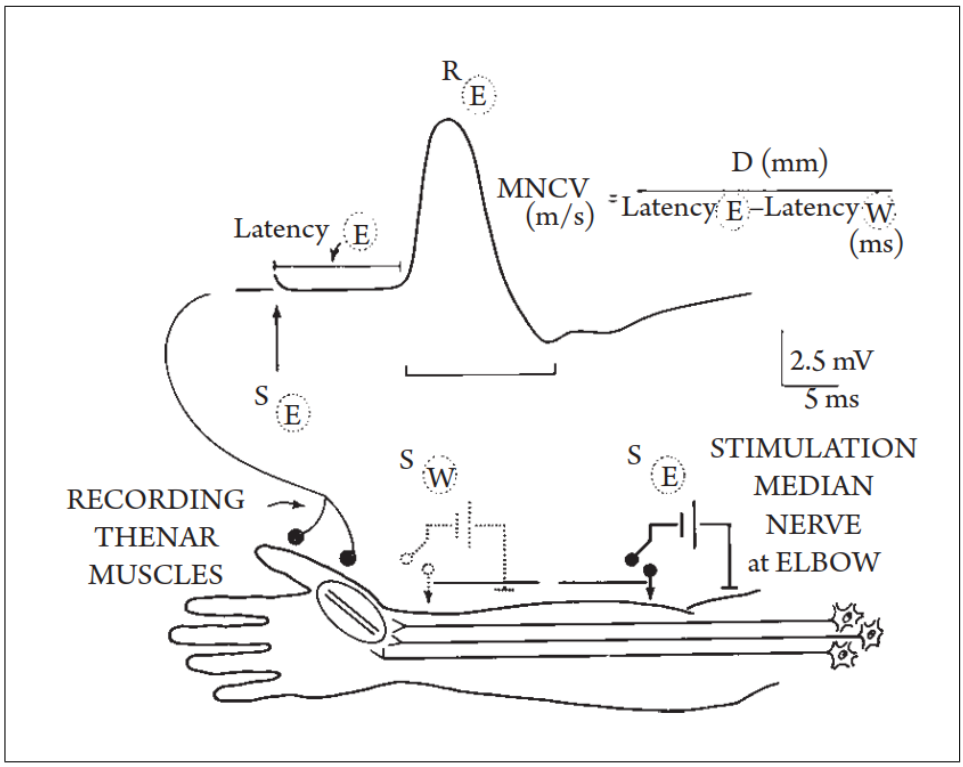

Figure 2.17 CMAP recorded from the thenar eminence(D, distance; S, signal; R, response; W, wrist; E, elbow)[75].

The electrodes are applied to the skin over the targeted nerves while the patient is lying down on an examination table during the test. The electrodes then record the electrical activity that results from stimulating the nerve with a modest electrical current. To acquire precise assessments of the latency and amplitude for each neuron, the test is performed numerous times.

The test may cause a slight tingling or discomfort for the patient, but it is normally painless and non-invasive (or minimally invasive). The electrodes are taken out after the test, and the skin is then cleansed with an alcohol swab. The test's outcomes, which are used to identify and assess diseases that impact the peripheral nervous system, are normally available within a few days.

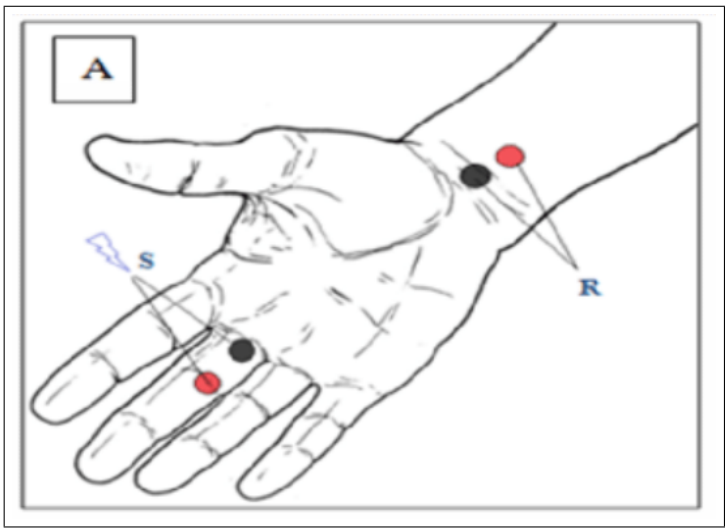

Figure 2.18 SNAP recorded from the middle finger (R, recording site; S, stimulation site)[79].

2.5.3 Applications of Nerve Conduction Studies

In a number of clinical contexts, nerve conduction investigations are performed to identify and assess diseases that have an impact on the peripheral nervous system. The following are only a few of the NCS's most widespread uses:

- Peripheral neuropathies: NCS can aid in the diagnosis and classification of several forms of peripheral neuropathies, including diabetic neuropathy, hereditary neuropathies, and neuropathies connected to autoimmune illnesses. The test can also be used to track how these conditions change over time [80].
- Nerve damage: NCS can be used to evaluate the severity and scope of nerve damage, such as that which results from trauma or surgery. The test can also assess the recovery of nerve function and assist in making treatment decisions.
- Myopathies: NCS can assist in the diagnosis and classification of certain muscle diseases, including muscular dystrophy, myasthenia gravis, and myotonic dystrophy. The test can also be used to track how these conditions change over time [81].
- Radiculopathies: Using NCS, it is possible to identify and localize nerve root

lesions that lead to radiculopathies, such as those brought on by herniated discs or spinal stenosis [82].

- CTS is a common condition that produces tingling, numbness, and discomfort in the hand and wrist. NCS may assist diagnose and assess CTS [36].

Overall, NCS are a valuable tool for diagnosing and evaluating conditions that affect the peripheral nervous system. These tests are safe, non-invasive, and provide important information about the function of the nerves and muscles in the body.

3. MATERIALS AND METHODS

3.1 Participants

Nineteen female patients and one male patient (age: 33-61) took part in this study. All participants have been diagnosed with unilateral early stage CTS (See Section 4.6 for further detail). The hand that is not affected by CTS is considered as control hand. Seven people had CTS in their left hand, while the rest had CTS in their right hand. The study was approved by Health Sciences University Kanuni Sultan Süleyman Training and Research Hospital Clinical Research Ethics Committee with an application number of 2021.06.196. All subjects signed the consent form. To prevent influencing the outcomes, participants were chosen not to have any other neurological or dermatological conditions.

3.2 Experimental Setup

The ultrasound actuated mid-air tactile stimuli were generated by Ultrahaptics STRATOS Explore device which is shown in Figure 2.1. The suggested optimal distance from the device use was 20 cm above the device according to Raza's paper [21]. However, I designed a stand with adjustable height to have that freedom for future works or experiments which can be seen in Figure 3.2. The mid-air ultrasound haptic stimuli expected to have an ellipsoid shape at the vertical central line [20], but the shape is expected to elongate in other directions when we are not at the vertical central line, as shown in Figure 3.1. In this experiment, any sound cues generated by device were masked by white noise presented to the participant's ears through headphones.

At the top of the stand there is an opening of the apparatus closed by plexiglass cover which has two different sized openings (55 mm and 23 mm) for each experiment, as shown in Figure 3.2. Experiment room is shown in Figure 3.5.

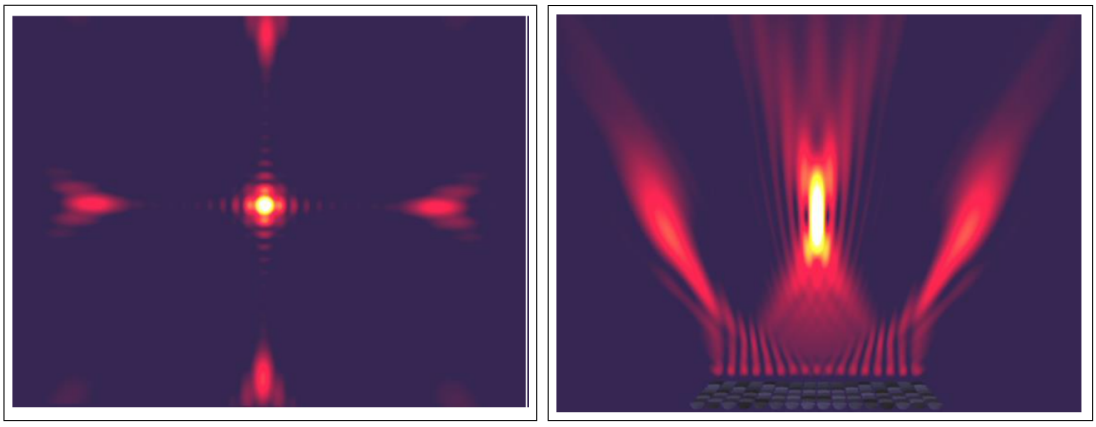

Figure 3.1 Visualization of an ultrasound focal point. Top-down perspective (left). Side Perspective (right) [20].

Figure 3.2 Apparatus (left) and the hand rest (right).

3.3 Stimuli and Procedure for Psychophysicsal Experiments

In the experiment, the burst of sine waves is used, as shown in Figure 3.3. The total duration of the stimulus was 2 seconds. Having a 50 ms rise and fall time. The burst duration at half-power point is 0.5 seconds. The stimuli had a frequency of 250 Hz. Ultrahaptics integrated development environment (IDE) software requires a sound file (.wav) to be called during the stimulus interval. The sound file (.wav) is created with MATLAB R2022a software.

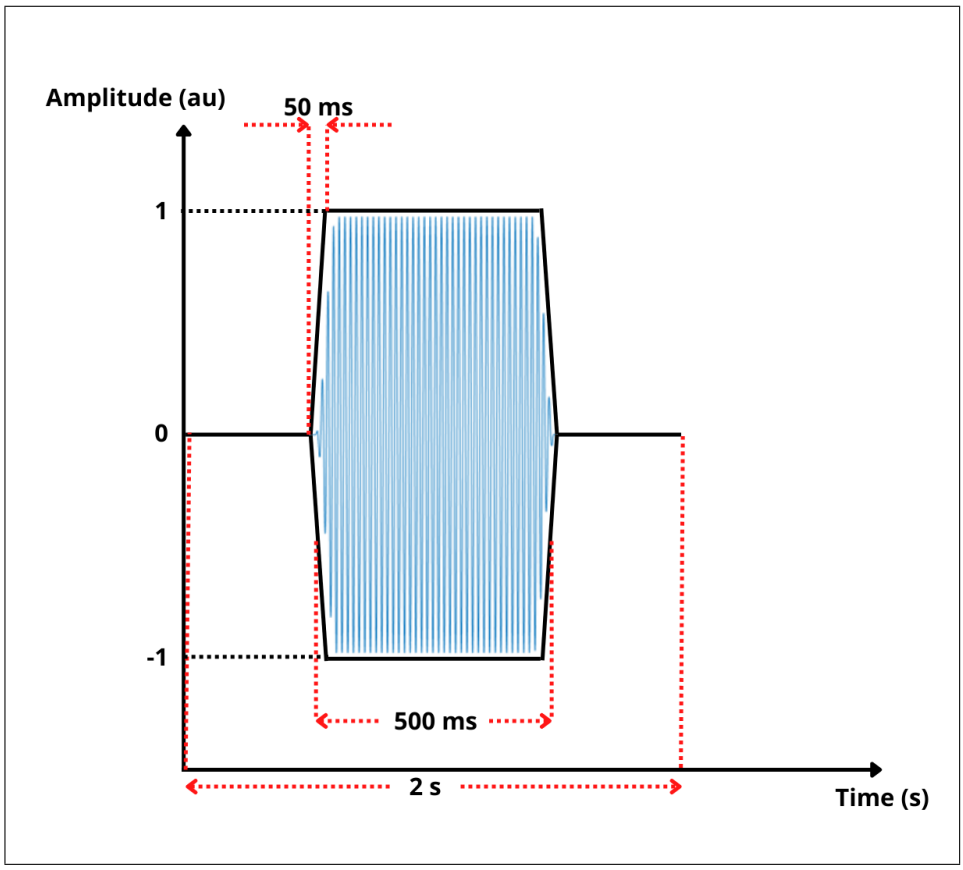

Figure 3.3 Stimulus used in the experiments.

The experiments utilized the two-alternative forced choice task (2-AFC), which minimizes participant bias during stimulus detection. The outcomes are therefore independent of the participant's criterion that would influence false-positive and false-negative responses [83]. The purpose of the participant is to determine whether the test stimulus occurred during the first or second interval. The test stimulus levels were dynamically changed during the experiment by using an up-down rule that resulted thresholds at 0.75 correct probability of detection [84]. According to the up-down rule, participant tries to guess the stimulus interval. For the correct answers, after getting 3 correct answer (not necessarily consecutive), the stimulus intensity is decreased by the a step size of 0.1 au, and for the first incorrect answer, the stimulus intensity is increased by a step size of 0.1 au. After the first incorrect answer, the step size is decreased to 0.02 au until the end of the experiment. After oscillating between ± 0.02 au for 20 trials, the absolute threshold value is set to that intensity level. Time diagram of the experiment can be seen in Figure 3.4.

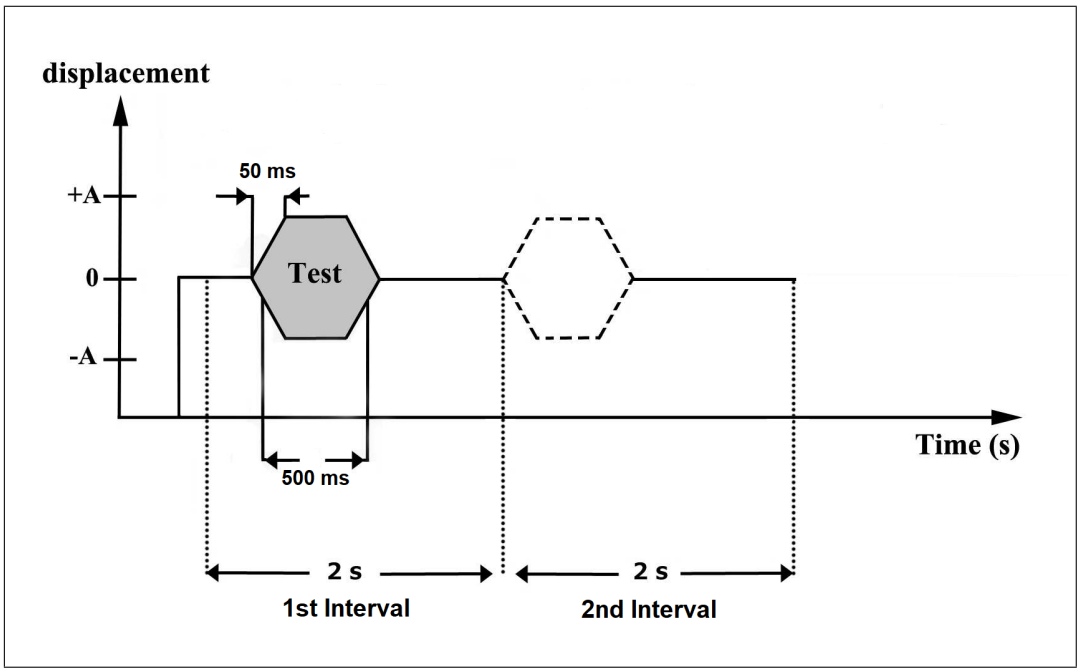

Figure 3.4 Time diagram of the experiment. The stimulus is either presented in the first or second interval [83].

Absolute thresholds of the participant are measured at 250 Hz modulation frequency for both D2 finger and thenar eminence part of the hand. A single focal point (8.6 mm radius) has been created on the skin surface. The 250 Hz modulated ultrasound vibration is expected to stimulate the Pacinian channel most on the hand around threshold level. Two experiment sessions were required for each hand (for D2 finger and thenar eminence). For participants both hands were tested, experiment session took less than 1 hour including the instructions, preparation of hands and breaks between the sessions.

3.4 System Usability Scale Questionnaire

The industry-accepted metric for assessing the usability of websites and products is the SUS score. The SUS scale, which stands for System Usability Scale, was developed by John Brooke in 1986. At first, it was mainly used for the new computing systems [85]. However, before long, the SUS was already being used in different kind of areas. In the questionnaire, participants need to answer 10 questions which was

Figure 3.5 Experiment room.

related with the system's usability. Each question has 5 different kind of responses that represent how strongly the participant agrees or disagrees. The scale's simplicity is what gives it its potency. It takes only a few minutes to finish the assessment. Even with only two participants, you may still learn a lot, however it is advised to have 8 to 20. The terminology employed in the scale is applicable to a wide range of systems, including digital software, websites, and physical objects. The correlation between the questionnaire and the SUS score is an important point to note. Individual questionnaire responses are not intended to be judged on their own. A single unit of measurement called the SUS Score is obtained by a series of computations.

There are several steps involved in converting questionnaire results into a SUS score. The questions with odd numbers inquire about the system's advantages, while those with even numbers inquire about its drawbacks. This was done on purpose to stop people from mechanically answering with the same number. For odd-numbered questions "User rating - 1", for even-numbered questions "5 - User rating" represents their scores. After adding the scores which will give a score out of 40, it is multiplied

by 2.5 to give a score out of 100. Even if the SUS is given out of 100, it should be noted that it is not a percentile. Actually, the SUS of 68 is around 50th percentile. SUS to percentile chart [85] was used to transform SUSs into corresponding percentile ranks.

3.5 Boston Carpal Tunnel and Visual Analog Scale Questionnaire

Boston Carpal Tunnel Questionnaire (BCTQ) contains two different sub-scales known as the Symptom Severity Scale (SSS) and the Functional Status Scale (FSS). The SSS gives information about the severity of the symptoms, on the other hand, the FSS generates a score about how proper the hand functions [86]. The SSS has 11 items whereas the FSS has 8 items. Each item receives a score between 1 and 5 (no symptoms to worst symptoms). After gathering scores for each questions, the mean value is calculated to give a final score for each sub-scales.

Visual Analog Scale (VAS) is a psychometric response scale that can be utilized in questionnaires. It is a measurement tool for subjective qualities or attitudes that cannot be measured directly. In VAS questionnaire, there is a 10-centimeter ruler, where patients are needed to pick a proper point depending on the severity of their symptoms. Being closer to start point (0 cm) means no symptoms, whereas being closer to the endpoint (10 cm) stands for worst symptoms. This questionnaire provides a score out of 10 for pain intensity.

3.6 EMG and Nerve Conduction Study Recordings

Electroneuromyography (ENMG), which was performed by Hatice Seğmen, M.D., specialist in neurology, was used to determine whether or not any of the subjects had CTS. The participants' ENMG findings determined that they had CTS, therefore that diagnosis was applied to them. Nerve conduction investigations, also known as NCS,

were carried out on the individuals' upper limbs while they were laying down in a posture that was most comfortable for them. All of the research was carried out at the typical room temperature of 25 degrees Celsius. The temperature of the hand's skin was kept at or above 32 degrees Celsius at all times. NCS were carried out with the use of a device known as the Neuropack S1 MEB-9400 (Nihon Kohden, Japan). In the upper extremities, the compound muscle action potential (CMAP) and sensory nerve action potential (SNAP) of the median and ulnar nerves were assessed. Over the abductor pollicis brevis (APB) muscle, median nerve stimulation was administered 8 centimeters proximal to the active recording electrode in order to record the median compound muscle action potentials (CMAPs). It was determined by measuring both the onset latency and the baseline-to-peak amplitude of the CMAPs. Orthodromic stimulation was used to obtain the median sensory nerve action potentials (SNAPs). The stimulation was applied to the palm and the third finger, and the recordings were made at the wrist. For every measurement, the onset latency, the peak-to-peak amplitude, and the conduction velocity were all recorded. In addition to this, the number of anomalous NCS findings for each participant as well as the number of nerves that were detected to be abnormal in any of the NCS measurements (onset latency, peak-to-peak amplitude, and conduction velocity) were counted. The data was analyzed using the published reference values that are recognized by Kanuni Sultan Suleyman Hospital EMG laboratory [75]. Electrode positionings can be seen in Figure 3.6.

Figure 3.6 Electrode positionings during NCS. An example setup for recording CMAP (left). An example setup for recording SNAP (right).

3.7 Virtual Reality-Assisted Hand Exercise Program

Fifteen female participants (age: 33-66) who were diagnosed with unilateral early stage CTS took part in this exercise program. In our Unity exercise game, participants need to complete a series of hand exercises consist of four sections, as shown in Figure 3.8. This exercise program has been prepared following the exercise program outline used by the American Academy of Orthopaedic Surgeons [87]. In each section, there are certain hand poses that the user needs to maintain for a certain amount of time to complete the exercise (see below). Additionally, if the user fails to maintain the hand pose for a certain amount of time (see below), the program continues with the next phase. The next phase can either be the next exercise or the next repetition in an exercise section.

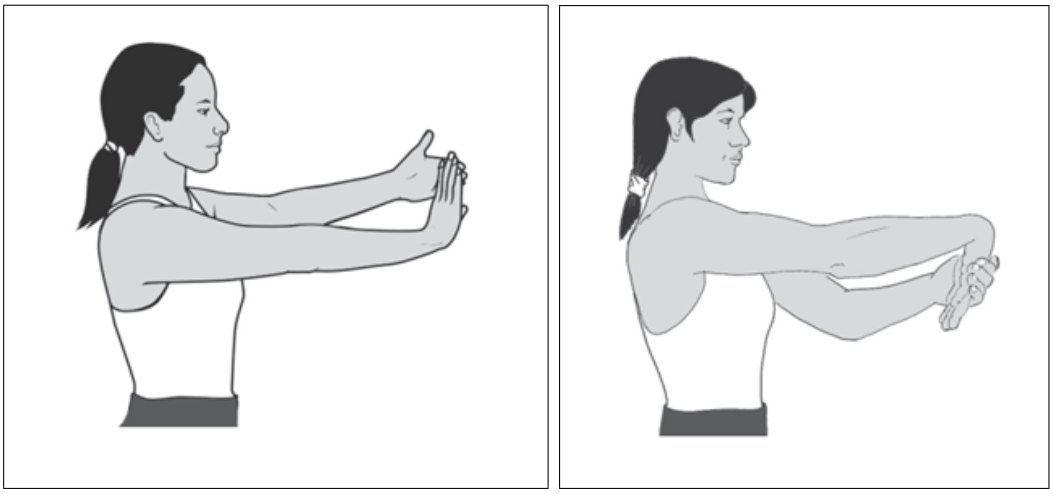

Figure 3.7 Wrist extension stretch (left) and wrist flexion stretch (right) hand exercises [87].

The performance scores for each section are calculated according to how long the user maintains the required hand exercise pose. For example, in Section 1, Wrist Extension Stretch, the whole exercise takes 75 seconds to finish (15 seconds for each repetition x 5). If users can maintain the pose perfectly for this duration, they get 75 points from that section.

Considering all stages of the exercise, a performance score can be as high as 330. The summary of the exercise program is shown below:

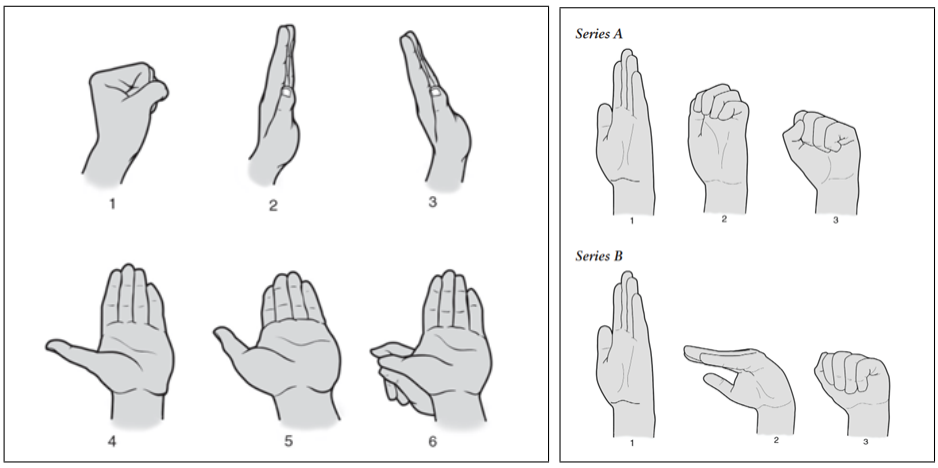

Figure 3.8 Medial nerve glides (left) and tendon glides (right) hand exercises [87].

1. Wrist Extension Stretch: 15 seconds x 5 repetitions = total of 75 points.
2. Wrist Flexion Stretch: 15 seconds x 5 repetitions = total of 75 points.
3. Medial Nerve Glides: 6 phases x 5 seconds each x 3 repetitions = total of 90 points.
4. Tendon Glides: 6 phases x 3 seconds each x 5 repetitions = total of 90 points.

For the wrist extension and flexion stretch part if the user fails to maintain the required hand pose for 10 seconds, the program continues with the next phase, this time limit is set to 5 seconds for the medial nerve and tendon glides part. After gathering all points for each section, the performance score is scaled to give a score out of 100. The formula for calculating the performance score is given in Eq. 3.1:

$$PerformanceScore = ((WES + WFS + MNG + TG)/330) * 100\% \tag{3.1}$$

where:

WES: wrist extension stretch score

WFS: wrist flexion stretch score

MNG: medial nerve glides score

TG: tendon glides score

At the start of the experiment, to ensure that the Leap Motion Controller is working in its ideal interaction zone, mid-air haptic feedback is given to the user above the 20-cm range of the Ultrahaptics array. Patients are asked to keep their hands at that distance from the device. By implementing this, we got rid of any unnecessary physical indicators that would distract the user while exercising. Additionally, at the end of each repetition, patients are also informed with mid-air haptic feedback pulse feedback to inform that they have completed the current exercise phase, which is implemented to enhance the user experience during the exercise.

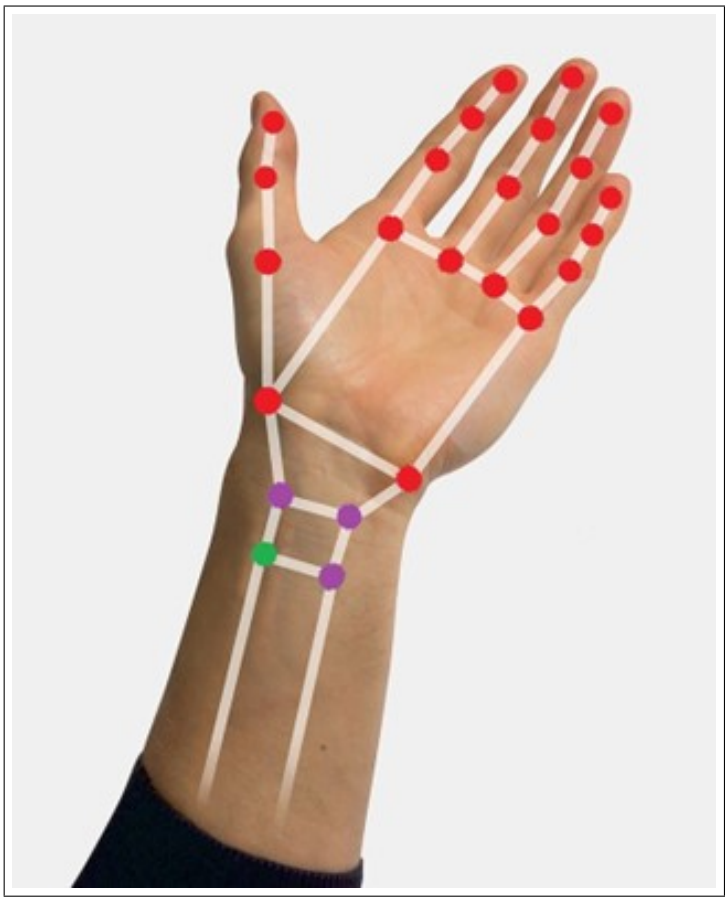

Figure 3.9 Hand model used in the exercise game.

Before starting the exercise, with the help of an instructor, each patient needs to save ideal hand position data for each exercise position. Due to the nature of the Leap Motion Controller, the size of the hand may affect how the program and the sensor

perceive the hand, and the device creates different hand models. For this particular reason, each patient will have their own ideal hand pose model. Those models will be used as target pose, and will be compared with the actual hand pose to decide whether the hand pose is suitable for the exercise or not. As we see in Figure 3.9, the red points (n = 21) on the hand are labeled as moving points, while the green one is labeled as a fixed point. During the exercise, the distance from each red point to the green point is calculated and used in real-time.

$$RMSE = \sqrt{\frac{1}{21}\Sigma_{i=1}^{21}\left(d_{Target_i} - d_{Actual i}\right)^2} \tag{3.2}$$

where:

d_{Target_i}: distance between the green point and the i^{th} red point saved in the model pose(m)

$d_{Actual i}$: distance between the green point and the i^{th} red point calculated in real-time(m)

Target distance values come from the model, which is unique for each user, and actual distance values are gathered in real-time. At the start of the exercise, each unique model for each exercise is created once and then saved for future use. When the RMSE value in Eq. 3.2 is above a certain limit (0.005 meter according to Unity3D [88]), an upper limit value selected after many trials, the program realizes that this hand pose is not suitable for this exercise and gives feedback to the user. If the user is able to fix the hand pose within the required time limit, the program continues to count down the timer and after the countdown next exercise begins. If the user fails to maintain the hand pose within time limit, the current point is saved for this session and program continues with the next exercise.

3.8 Data Analysis

The statistical analysis was done using MATLAB R2022a. The absolute threshold values of thenar eminence for both the CTS affected hand and the healthy control hand were compared with an unpaired t-test. The Pearson correlation coefficients were being calculated for comparing the results.

4. RESULTS

4.1 Psychophysical Results for the Thenar Eminence

All participants completed the psychophysical experiments. Absolute threshold values were measured for the thenar eminence in both hands. The unaffected hand was considered as the control hand. The unpaired t-test was used to compare two hand: the hand affected by CTS (M=0.85 au, SD=0.15) and the healthy hand (M=0.87 au, SD=0.16). The t-test yielded, t(38) = 0.3938, p = 0.70. According to this result, statistically no significant difference found between the two hands. The data distribution of CTS affected hand and healthy hand is shown in Figure 4.1 and 4.2.

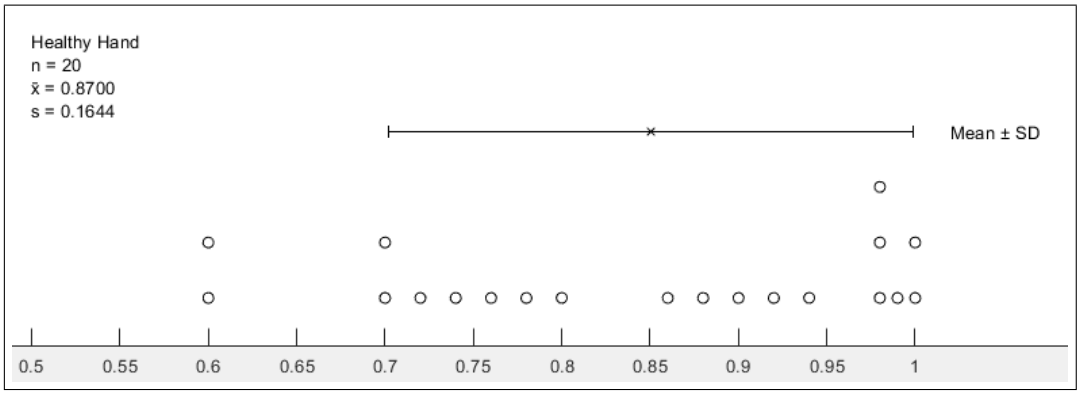

Figure 4.1 Healthy hand absolute threshold distribution (au) for thenar eminence area.

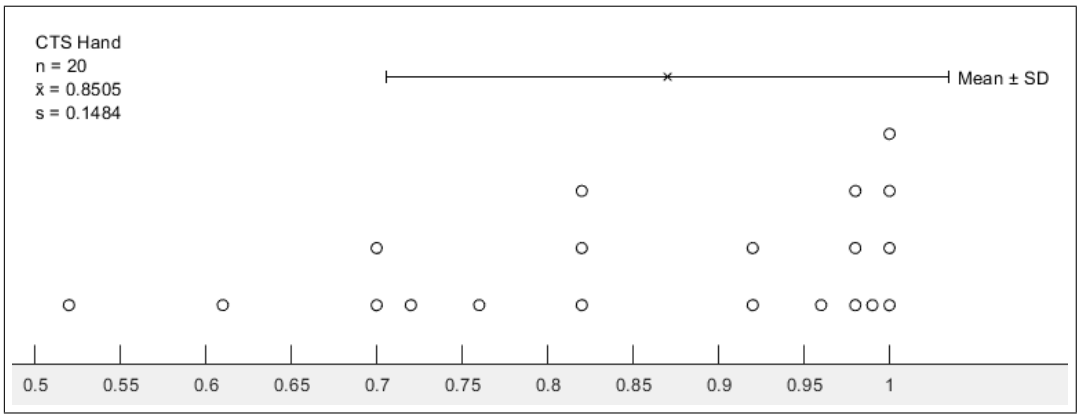

Figure 4.2 CTS affected hand absolute threshold distribution (au) for thenar eminence area.

4.2 Psychophysical Results for the D2 Finger

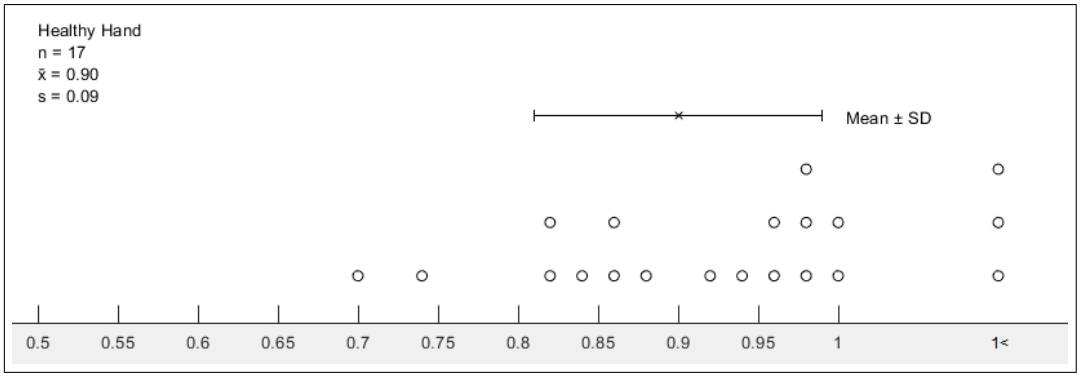

Figure 4.3 Healthy hand threshold values for D2 finger (au).

Same patients from the previous thenar experiment also participated in this experiment. Absolute threshold values were measured for the D2 fingertip area in both hands. The patients were diagnosed with unilateral early stage CTS. The unaffected hand is used as the control hand. For the affected hand, none of the patients out of twenty could feel the ultrasound stimulus, whose intensity level was equal to the device's upper boundary. Due to safety concerns, the intensity level was not increased beyond the upper boundary, which is equal to 1.00 au for the device. For the unaffected hand, seventeen patients out of twenty were able to get a threshold value between 0 and 1.0 au (M=0.90 au, SD=0.09) which is shown in Figure 4.3. The remaining patients could not feel the stimulus, so they were expected to have a threshold level above 1.0 au.

4.3 System Usability Scale Results for the Virtual Reality-Assisted Hand Exercise Program

Fifteen female participants between the ages of 33 and 66 who were diagnosed with unilateral early stage CTS took part in this exercise program. After completing the virtual reality-assisted hand exercise program, each participant was asked to complete a system usability scale survey to assess the usability of the exercise program. A SUS above 68 is considered above average (50th percentile) [85]. According

to our sample group, the average SUS for this exercise program was obtained as 80.17 (between 85-89th percentile). SUS of each participant can be seen from the Figure 4.4. After conducting a one-tailed t-test for our SUS result (M=80.17%, SD=18.33) and comparing them with the average score of 68 (50th percentile), the results were calculated as: $t(14) = 2.57$, $p = 0.011$. The results show that we can be around 99% confident that this exercise program has an average score greater than the literature average of 68.

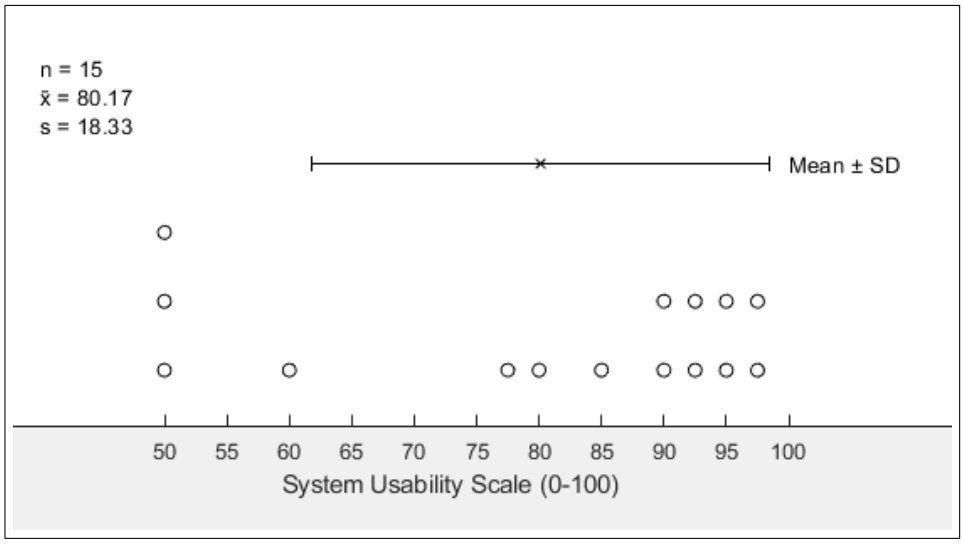

Figure 4.4 System usability scale results.

4.4 Performance Scores for the Virtual Reality-Assisted Hand Exercise Game

VR-assisted hand exercise game performance scores (M=83.31%, SD=14.80) of each participants are shown in Figure 4.5. These scores are used to check correlation between the system usability scores. After conducting the test, Pearson correlation coefficient value calculated as $\rho = 0.89$, $p < 0.001$. The correlation result shows that there is a significant correlation between SUS and performance scores, which will be discussed in chapter 5. After conducting a one-tailed t-test for our performance score results (M=83.31%, SD=14.80) and comparing them with the average score of 50, the results were calculated as: $t(14) = 8.71$, $p < 0.001$. The results show that we can

be more than 99% confident that the patients has an average score greater than the performance score of 50.

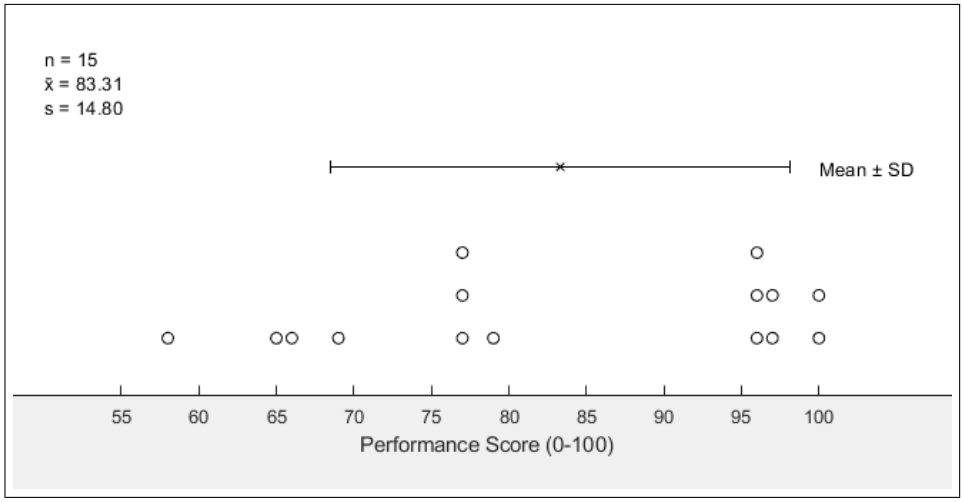

Figure 4.5 Performance score results.

4.5 Boston Carpal Tunnel and Visual Analog Scale Questionnaire Results

The 20 CTS patients that took part in the physchophysical experiments filled out Boston Carpal Tunnel Questionnaire (BCTQ) and visual analog scale (VAS) questionnaire before the experiment session. The results for 20 patients' BCTQ and VAS questionnaire results are shown in Table 4.1. According to the literature, a VAS score between 0 to 0.50 cm indicate no pain, 0.50 to 4.50 cm indicate minor pain, 4.50 to 7.50 mm indicate moderate pain, and 7.50 cm to 10 cm indicate severe pain [89]. Comparing these scores with the VAS scores given in the Table 4.1, our patients fit into moderate pain category (4.5-7.5 VAS score) after conducting one-tailed t-test to check the upper boundary score of 7.5, $t(19) = 3.06$, $p = 0.003$, we are almost 100% confident that the patients has an average VAS score less than the upper boundary of 7.5 score.

Also, Sarilar et. al measured both FSS and SSS scores for CTS patients ($n = 106$) with severity scales normal (grade 0), mild (grade 2), moderate (grade 3), and severe (grade 4) [90]. According to their results, grade 0 patients have FSS ($M = 2.3$,

SD = 1.0) and SSS (M = 2.5, SD = 0.8), grade 2 patients have FSS (M = 2.7, SD = 1.1) and SSS (M = 2.8, SD = 0.9), grade 3 patients have FSS (M = 2.9, SD = 1.2) and SSS (M = 3.1, SD = 0.8), and grade 4 patients have FSS (M = 3.6, SD = 1.3) and SSS (M = 3.9, SD = 0.8). Comparing these results with our findings, in our sample group the gap between the SSS score and FSS score is larger than expected, which may be linked to the sample size (n = 20).

Table 4.1
Mean (M) and standard deviations (SD) of Boston Carpal Tunnel Questionnaire and Visual Analog Scale Questionnaire data.

	M	SD
VAS	6.50	1.46
Boston SSS	2.65	0.49
Boston FSS	1.98	0.58

4.6 EMG and Nerve Conduction Study Results

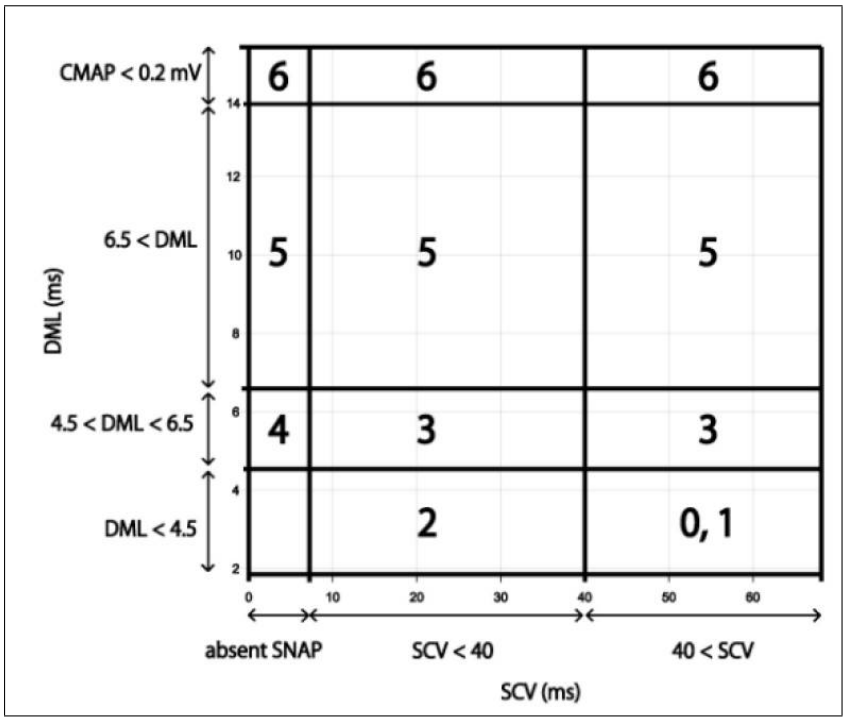

Figure 4.6 CTS severity grades; where, SCV: sensory conduction velocity, DML: distal motor latency [91].

The 20 patients that took part in the physchophysical experiments were selected according to their severity of the CTS. According to the severity classifications in literature, grade 1 (very mild) patients are the ones who have orthodromic sensory conduction velocity (SCV) higher than 40 m/s and distal motor latency (DML) less than 4.5 ms. grade 2 (mild) patients are the ones who have orthodromic SCV less than 40 m/s and DML less than 4.5 ms [91, 92]. Half (n = 10) of our CTS patients fall into the grade 1 category with SCV (M = 41.53 m/s, SD = 1.07) and DML (M = 3.48 ms, SD = 0.27), while the other half (n = 10) falls into the grade 2 category with SCV (M = 36.00 m/s, SD = 2.92) and DML (M = 3.62, SD = 0.23).

The EMG and NCS results are summarized in Table 4.2, and the explanations for the recordings are presented below:

Table 4.2
Mean (M) and standard deviations (SD) of EMG and nerve conduction study data.

	M	SD
Median Sensory Latency 1 (ms)	2.92	0.41
Median Sensory Latency 2 (ms)	3.73	0.51
Median Sensory. Amplitude (mV)	12.2	5.84
Median Sensory Conduction Velocity (m/s)	38.7	3.55
Motor Latency Wrist (ms)	3.55	0.25
Motor Latency Elbow (ms)	7.54	0.43
Motor Amplitude Wrist (mV)	7.59	1.69
Motor Amplitude Elbow (mV)	7.52	1.72
Motor Conduction Velocity (m/s)	56.9	4.99

- Median Sensory Latency 1 (Wrist): Stimulating ring electrodes are connected to the D3 finger; recording electrodes are connected to a region close to the wrist (Distal sensory latency).

- Median Sensory Latency 2 (Elbow): Stimulating ring electrodes are connected to the D3 finger; recording electrodes are connected to a region close to the elbow (Proximal sensory latency).

- Median Sensory Conduction Speed: (distance between the proximal and distal stimulation sites) divided by (proximal sensory latency - distal sensory latency)
- Median Motor Latency (Wrist): Stimulating electrodes are connected to the wrist; recording electrodes are connected to the APB muscle in the thenar area (Distal motor latency).
- Median Motor Latency (Elbow): Stimulating electrodes are connected to the elbow; recording electrodes are connected to the APB muscle in the thenar area (Proximal motor latency).
- Median Motor Amplitude (Wrist): Stimulating electrodes are connected to the wrist; recording electrodes are connected to the APB muscle in the thenar area.
- Median Motor Amplitude (Elbow): Stimulating electrodes are connected to the elbow; recording electrodes are connected to the APB muscle in the thenar area.
- Median Motor Conduction Velocity: (distance between the proximal and distal stimulation sites) divided by (proximal motor latency - distal motor latency)

4.7 Correlation Results Between Questionnaires, EMG, NCS, and Thenar Eminence Threshold for Ultrasound Stimulus

The pearson correlation coefficients and their corresponding p values between EMG & NCS Data versus thenar eminence threshold for ultrasound stimulus is shown in Table 4.3; however, there is no significant correlation between the parameters. In Table 4.4, we also cannot see any strong correlation between the TE threshold for ultrasound stimulus data vs BCTQ & VAS questionnaire. The same applies to the Table 4.5 and Table 4.6.

Table 4.3
Pearson correlation coefficients (rho) and their corresponding p values between EMG & NCS Data vs Thenar Eminence Threshold for Ultrasound Stimulus.

	TE Ultrasound Threshold	
	Rho	P
Sensory Latency 1	0.134	0.572
Sensory Latency 2	0.261	0.266
Sensory Amplitude	-0.273	0.243
Sensory Conduction Velocity	-0.191	0.419
Motor Latency Wrist	-0.077	0.745
Motor Latency Elbow	0.197	0.404
Motor Amplitude Wrist	0.162	0.494
Motor Amplitude Elbow	0.178	0.451
Motor Conduction Velocity	-0.358	0.121

Table 4.4
Pearson correlation coefficients (rho) and their corresponding p values between VAS & Boston Questionnaires vs Thenar Eminence Threshold for Ultrasound Stimulus.

	TE Ultrasound Threshold	
	Rho	P
VAS	-0.130	0.582
Boston FSS	-0.203	0.388
Boston SSS	-0.394	0.085

Table 4.5
Pearson correlation coefficients (rho) and their corresponding p values between EMG & NCS Data vs VAS & Boston Questionnaires.

	VAS		Boston FSS		Boston SSS	
	Rho	P	Rho	P	Rho	P
Sensory Latency 1	-0.141	0.551	0.206	0.383	0.134	0.570
Sensory Latency 2	-0.142	0.550	0.112	0.635	0.073	0.759
Sensory Amplitude	0.139	0.557	0.532	0.015	0.272	0.244
Sensory Conduction Velocity	0.102	0.667	-0.076	0.749	-0.081	0.733
Motor Latency Wrist	-0.177	0.454	-0.012	0.959	0.167	0.479
Motor Latency Elbow	-0.312	0.179	0.012	0.958	-0.188	0.425
Motor Amplitude Wrist	-0.032	0.890	0.230	0.328	-0.023	0.923
Motor Amplitude Elbow	-0.019	0.933	0.157	0.508	-0.066	0.781
Motor Conduction Velocity	-0.054	0.819	0.056	0.814	0.162	0.494

Table 4.6
Pearson correlation coefficients (rho) and their corresponding p values between EMG & NCS Data vs SUS & Performance Scores.

	SUS		Performance Score	
	Rho	P	Rho	P
Sensory Latency 1	-0.143	0.611	-0.154	0.582
Sensory Latency 2	-0.006	0.982	-0.080	0.776
Sensory Amplitude	0.104	0.711	0.174	0.533
Sensory Conduction Velocity	0.404	0.134	0.375	0.168
Motor Latency Wrist	-0.127	0.649	-0.196	0.481
Motor Latency Elbow	-0.285	0.302	-0.138	0.622
Motor Amplitude Wrist	0.067	0.810	0.023	0.935
Motor Amplitude Elbow	-0.021	0.938	-0.024	0.930
Motor Conduction Velocity	0.280	0.311	0.305	0.268

5. DISCUSSION

5.1 Previous Studies

According to the studies in the literature, medical ultrasound imaging and nerve conduction studies are proven techniques for the diagnosis of CTS. Elnady et al. used high resolution ultrasound (HRUS) to assess median nerve cross-sectional area, and as a result they reported that HRUS is a promising tool that can label CTS and its severity with good accuracy [93]. Georgiev et al. also used medical ultrasound imaging for the diagnosis of CTS [94]. According to their paper, the sonographic method has a number of benefits, including the following: it is readily available, it does not involve any invasive procedures, it is less expensive, it makes the evaluation and diagnosis of CTS simpler and more expedient, and it provides the opportunity to evaluate a number of parameters of the median nerve, such as its size, blood flow, and mobility [94]. According to the study by Wiesler et al., at the level of the distal wrist crease, the area of the median nerve's cross-section was assessed in CTS patients as well as in healthy controls [95]. Their results show that high-resolution ultrasound is useful for diagnosing CTS and that the median nerve gets bigger at the distal wrist crease in people who have symptoms [95]. In their paper, Yoshii et al. reviewed the recent advancements in CTS diagnosis based on ultrasound dynamic images and discussed its pathology [37]. They also indicate that the static ultrasound measurement of the median nerve cross-section area may eliminate the need for electrophysiological testing [37].

In contrast, the Ultrahaptics STRATOS Explore device can be accessed from any location and does not require a medical evaluation as is the case with the other methods we've discussed so far, which can only be performed in a hospital or other medical facility.

Furthermore, mid-air haptic sensation produced by ultrasound actuators has

been implemented as a tactile interface in medical training simulators. For example, in their study, Balint et al. combined virtual reality, palpation and ultrasound mid-air haptic system to enhance palpation training and its outcome [96]. Their results show that the mid-air haptic sensations implemented in VR applications have great potential to increase the user experience with a low-cost setup. Also another application of mid-air haptic sensation in medical use is generating Braille code in mid-air for visually impaired individuals, where 90 percent accuracy rate can be achieved [97].

In the literature, there are many studies about virtual-reality assisted exercise programs. Those programs mainly try to enhance the user experience by implementing virtual reality on top of a traditional exercise scheme. For example, Cho et al. investigated the effects of a virtual reality exercise program in hemodialysis patients [98]. They divided patients into two groups, one group using the VR exercise program while the other one received their usual care. According to their results, VR exercise program enhances hemodialysis patients' physical fitness, body composition, and fatigue more compared with the traditional methods. Finkelstein et al. examined the effects of VR exercise games on children with autism [99]. Exercise provides significant behavioral and physiological benefits to children with autism, despite the fact that many of these children lead sedentary lifestyles. According to their results, most of the participants showed intense levels of effort and they stated that they would exercise more if they had access to this kind of exercise games more [99]. Another study has been done by Park et al. about enhancing the balance and gait of elderly people by conducting virtual reality exercise instead of traditional ball exercise [100]. Their results showed that sway length of the patients were decreased more with virtual reality exercises compared to traditional ball exercise [100]. Additionally, Zeng et al. compared the traditional stationary exercise bike and virtual reality based exercise bike in terms of physiological and psychological responses after the exercise has been done [101]. Their results indicated that the traditional exercise bike yields better perceived exertion rates than the VR-based exercise bike; nevertheless, VR-based exercise biking sessions have higher levels of confidence and enjoyment compared with traditional sessions [101]. These studies show that the use of virtual reality in a wide variety of clinical and non-clinical applications has a great impact on enhancing the user experience.

Due to it being a brand new technology, there is no research about ultrasound mid-air haptic being used directly for CTS preliminary diagnosis and therapy. However, there are several studies related to the use of mid-air haptics in AR and VR applications [18, 102, 103].

5.2 Psychophysical Assessment of Carpal Tunnel Syndrome Patients

For the patients developing CTS; sensory fibers often are affected first, followed by motor fibers. For our study we have selected patients having early stages of CTS. Looking at the results given in the section 4.1, the threshold values for thenar eminence shows that we fail to say that the two groups are different from each other. The underlying reason behind this can be the branching of the median nerve before entering the carpal tunnel, as shown in Figure 5.1 [104]. The palmar cutaneous branch of median nerve (PCBm), providing sensory information from the skin to the brain, does not pass through the carpal tunnel. However, according to the studies in the literature, it is not possible to say that the PCB is not affected in patients with CTS. There are some studies showing that this branch is not an ideal comparator nerve branch for the diagnosis for CTS. In their study, Uluc et al. investigated the conduction of PCBm in patients with CTS [105]. According to their results, 56% of the CTS patients had abnormalities in their PCBm conduction. Also another study that is done by Rathakrishnan et al. reported that 46% of the CTS patients had abnormalities in their PCBm conduction [106]. This specific abnormality rate can be linked to injury to both of these nerves simultaneously [105]. In theory, it looks viable to say the sensory functions of the patients in thenar eminence area mostly not affected because the branching occurs before the carpal tunnel; however, in practice it is not the case.

Looking at the results given in the section 4.2, while all patients are having a threshold value higher than 1.0 Ultrahaptics amplitude unit at their affected hand for D2 fingertip area; for the hand that is not affected by CTS, most of them have

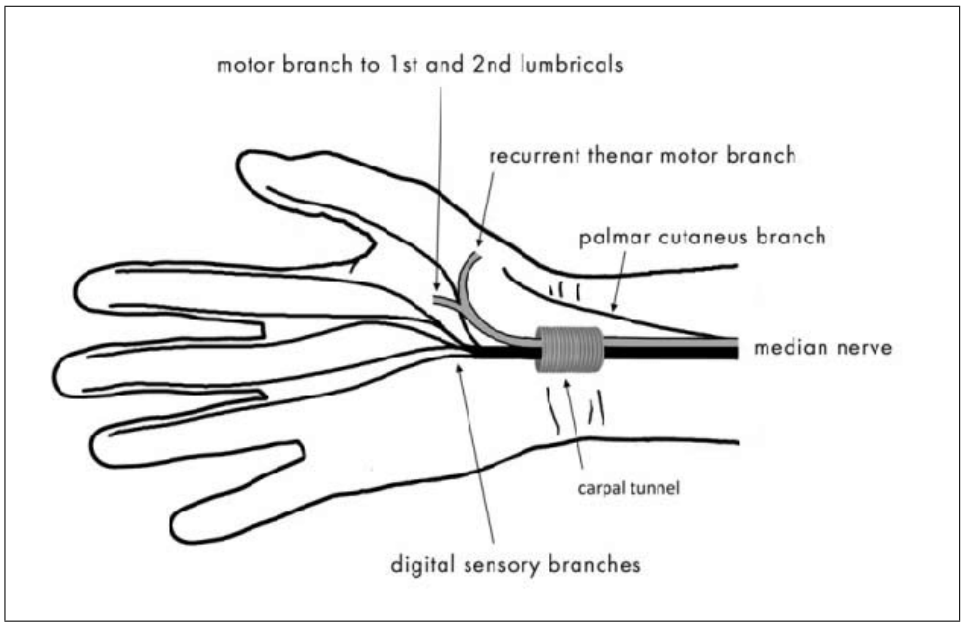

Figure 5.1 Branches of the median nerve and the carpal tunnel [107].

a threshold value between 0 and 1 for the same fingertip area. Although, it is not possible to conduct a statistical analysis without having the exact values of thresholds, we can easily say that not being able to feel the maximum amplitude that the device can output may indicate the early symptoms of the CTS.

The ultrasound mid-air haptic technology itself cannot replace the traditional CTS diagnosis methods, however it can be used for the preliminary diagnosis of the CTS if certain improvements and enhancements are made. The current maximum amplitude level is not viable for measuring a threshold value in patients with CTS; however, with the new transducers introduced on 2 November 2022 by Ultraleap company can be used in future studies to test whether their new maximum amplitude limit introduced by safety regulations are applicable for patients having sensory nerve damage. Supra-threshold experiments like intensity discrimination can also be implemented if the device is able to output higher amplitude levels than the currently available ones.

If the necessary improvements are made, being easily accessed from outside of a medical institution, makes this technology and the device a great tool for informing the society about CTS and it has an important place for early prevention and treatment

of CTS.

5.3 Usability of Virtual Reality-Assisted Hand Exercise Game

When the findings that were reported in Sections 4.3 and 4.4 are taken into consideration, a system usability score of 80.17 is considered to be above average and shows that the system is user-friendly, time-saving, and capable of effectively satisfying the requirements defined by its users. Users are more likely to be pleased with the system, which may result in higher engagement and sustained use, which is very key point for the CTS therapy. Sustaining the daily hand exercises can result in prolonging the surgery and even capable of improving the symptoms of the patients. In Section 5.1, the impact of using the VR technology in traditional systems has already been discussed, and with the help of adding another sensation to the system, the haptic sensation, the user experience is further enhanced.

The performance scores are also quite valuable pieces of information because they reflect the level of effort that patients put into their exercises. These scores can be saved for use in a future study to a cloud service, where the attending physician can track the progress of each patient and take appropriate action as necessary. It should not be disregarded that these advancements will have a significant impact on society as well as the therapy and treatment of patients with CTS.

In Section 4.5, after comparing the SUS and performance scores, we see that there is a strong correlation between them. It shows that patients who achieved a good performance score during their exercise gave a high score for the SUS questionnaire they filled out afterwards, even if they do not have access to their exercise performance scores. This situation shows the quality of the exercise creates a strong bias against the exercise system, which could affect the motivation and the effort put in by the patient.

5.4 Correlation Between Boston CTS Questionnaires, Thenar Eminence Threshold for Ultrasound Stimulus, VAS, EMG, and NCS

Looking at the results presented in Tables 4.3, 4.5, 4.5 and 4.6; we see that there is no significant correlation either in the positive or negative direction. According to a study done by Dhong et al. [108], they found that the NCS data correlated significantly ($p < 0.05$) with the Symptom Severity Scale score. They also stated that the correlation of the NCS with the Functional Status Scale was weaker compared with the SSS score. In our study, we could not find a statistically significant correlation between those two parameters. The underlying result behind this can be the sample size difference between the two studies because there were 138 patients (222 hands) in Dhong's study. Also, the affected hands of the CTS patients in Dhong's study had a much wider range (six different grades from 5 to 0: extreme, severe, moderate, mild, very mild, and negative) compared to our study (only grade 1 and grade 2 patients). Another study with a wide range of CTS patients done by Yang et al. [109] also confirms that the severity of the CTS that is measured by electrodiagnostic testing (EDT) has a positive correlation with the CTS 6 (CTS-6) score and Semmes-Weinstein Monofilament Test (SWMT) results. That result also supports the fact that the sample size and the low diversity of patients in terms of severity of CTS had a negative effect on our correlation results. However, it was not possible to pick patients from a much wider severity scales because of the limitations of the mid-air ultrasound device.

Additionally, the TE threshold for ultrasound stimulus has no statistically significant correlation with other results. This shows that the mid-air ultrasound technology cannot replace the traditional methods for the diagnosis of CTS, however as stated above, this technology can be used to point out the early symptoms of the CTS. Also being able to be accessed from anywhere makes this device and the technology a complementary pre-diagnostic tool rather than being a substitute.

5.5 Limitations

For this thesis project, the Stratos Explore device was mainly used for both psychophysical experiment implementations and virtual reality-assisted hand exercise program. The ultrasound haptics has some limitations that affected its use in this particular thesis project.

First thing comes to mind is its precision. The transducers that are used for this device transmits 40 kHz ultrasound waves that has 8.6 mm wavelength in air. The smaller wavelengths results in smaller focal points. Having a very small sized focal point is expected to enhance the quality of psychophysical experiments due to the fact that it will be easier to focus the stimulus on certain parts of the human hand.

The second factor that had an impact in this study was the perceptible strength of the ultrasound haptic signal. Each transducer has a tactile force around 0.016 N [110]. Combining it with other transducers increases the tactile force; however, addition of each transducer has a diminishing return. In other words, the tactile force is not increasing linearly with addition of new transducers because of the the positioning of the arrays. Some early-stage CTS patients could not feel the maximum output stimulus due to the combination of maximum amplitude limitations and their loss of sensation in the D2 finger, which caused them to not be able to measure the threshold values from the D2 finger. Using mixed transducer array, where there are several frequency types (40 and 70 kHz) are present has been shown to improve the total output force according to a study made by Ito et al. [111], which may improve the sensibility of the ultrasound haptic signal.

The range of the device is also limited. The optimum range is 20 cm away from the transducers, however it is not possible to work under 20 cm distance. Also the strength and accuracy is drastically decreasing for distances greater than 20 cm. This affects its applications where user needs to move his/her hands constantly. The psychophysical experiments carried out in this study are unaffected by this issue, but the patients participating in the hand exercise game felt restricted because of the small

effective working area provided by the device.

5.6 Future Work

To address the limitations, as future work, ultrasound arrays having different positions and angles for certain applications can be used to increase their effectiveness. Also the strength of the mid-air haptic vibration changes depending on its 3D location, higher the amplitude at the center and above 20 cm of the array, and lower the amplitude as we move further away from that area. For this problem, a research about the calibration of the device can be done to be able to uniformly distribute a certain amplitude for greater region. Also the bias that we have encountered during the exercise program can be investigated and avoided for enhancing the user experience and improving the quality of the exercise.

REFERENCES

1. Atroshi, I., C. Gummesson, R. Johnsson, and A. Sprinchorn, "Symptoms, disability, and quality of life in patients with carpal tunnel syndrome," *The Journal of Hand Surgery*, Vol. 24, no. 2, pp. 398–404, 1999.

2. Rempel, D. M., and E. Diao, "Entrapment neuropathies: pathophysiology and pathogenesis," *Journal of Electromyography and Kinesiology*, Vol. 14, no. 1, pp. 71–75, 2004.

3. Padua, L., D. Coraci, C. Erra, C. Pazzaglia, *et al.*, "Carpal tunnel syndrome: clinical features, diagnosis, and management," *The Lancet Neurology*, Vol. 15, no. 12, pp. 1273–1284, 2016.

4. Atroshi, I., C. Gummesson, R. Johnsson, E. Ornstein, *et al.*, "Prevalence of carpal tunnel syndrome in a general population," *Jama*, Vol. 282, no. 2, pp. 153–158, 1999.

5. Wipperman, J., and K. Goerl, "Carpal tunnel syndrome: diagnosis and management," *American Family Physician*, Vol. 94, no. 12, pp. 993–999, 2016.

6. Kozak, A., G. Schedlbauer, T. Wirth, U. Euler, *et al.*, "Association between work-related biomechanical risk factors and the occurrence of carpal tunnel syndrome: an overview of systematic reviews and a meta-analysis of current research," *BMC Musculoskeletal Disorders*, Vol. 16, no. 1, pp. 1–19, 2015.

7. Calandruccio, J. H., and N. B. Thompson, "Carpal tunnel syndrome: making evidence-based treatment decisions," *Orthopedic Clinics*, Vol. 49, no. 2, pp. 223–229, 2018.

8. Genova, A., O. Dix, A. Saefan, M. Thakur, *et al.*, "Carpal tunnel syndrome: a review of literature," *Cureus*, Vol. 12, no. 3, 2020.

9. Chen, K.-T., Y.-P. Chen, Y.-J. Kuo, and M.-H. Chiang, "Extracorporeal shock wave therapy provides limited therapeutic effects on carpal tunnel syndrome: A systematic review and meta-analysis," *Medicina*, Vol. 58, no. 5, p. 677, 2022.

10. Kothari, M. J., *et al.*, "Carpal tunnel syndrome: Clinical manifestations and diagnosis," *UpTodate[Online]*, 2020.

11. Limerick, H., R. Hayden, D. Beattie, O. Georgiou, *et al.*, "User engagement for mid-air haptic interactions with digital signage," in *Proceedings of the 8th ACM International Symposium on Pervasive Displays*, pp. 1–7, 2019.

12. Ultraleap, "World-leading hand tracking products: Small. fast. accurate.." Available at https://www.ultraleap.com/product/. Accessed: 2023-4-28.

13. Iwamoto, T., M. Tatezono, and H. Shinoda, "Non-contact method for producing tactile sensation using airborne ultrasound," in *Haptics: Perception, Devices and Scenarios: 6th International Conference, EuroHaptics 2008 Madrid, Spain, June 10-13, 2008 Proceedings 6*, pp. 504–513, Springer, 2008.

14. Harrington, K., D. R. Large, G. Burnett, and O. Georgiou, "Exploring the use of mid-air ultrasonic feedback to enhance automotive user interfaces," in *Proceedings of the 10th International Conference on Automotive User Interfaces and Interactive Vehicular Applications*, pp. 11–20, 2018.

15. Georgiou, O., C. Jeffrey, Z. Chen, B. X. Tong, *et al.*, "Touchless haptic feedback for vr rhythm games," in *2018 IEEE Conference on Virtual Reality and 3D User Interfaces (VR)*, pp. 553–554, IEEE, 2018.

16. Martinez, J., A. Harwood, H. Limerick, R. Clark, *et al.*, "Mid-air haptic algorithms for rendering 3d shapes," in *2019 IEEE International Symposium on Haptic, Audio and Visual Environments and Games (HAVE)*, pp. 1–6, IEEE, 2019.

17. Martinez, J., D. Griffiths, V. Biscione, O. Georgiou, *et al.*, "Touchless haptic feedback for supernatural vr experiences," in *2018 IEEE Conference on Virtual Reality and 3D User Interfaces (VR)*, pp. 629–630, IEEE, 2018.

18. Hwang, I., H. Son, and J. R. Kim, "Airpiano: Enhancing music playing experience in virtual reality with mid-air haptic feedback," in *2017 IEEE World Haptics Conference (WHC)*, pp. 213–218, IEEE, 2017.

19. Freeman, E., D.-B. Vo, and S. Brewster, "Haptiglow: Helping users position their hands for better mid-air gestures and ultrasound haptic feedback," in *2019 IEEE World Haptics Conference (WHC)*, pp. 289–294, IEEE, 2019.

20. Rakkolainen, I., E. Freeman, A. Sand, R. Raisamo, *et al.*, "A survey of mid-air ultrasound haptics and its applications," *IEEE Transactions on Haptics*, Vol. 14, no. 1, pp. 2–19, 2020.

21. Raza, A., W. Hassan, T. Ogay, I. Hwang, *et al.*, "Perceptually correct haptic rendering in mid-air using ultrasound phased array," *IEEE Transactions on Industrial Electronics*, Vol. 67, no. 1, pp. 736–745, 2019.

22. Rakkolainen, I., A. Sand, and R. Raisamo, "A survey of mid-air ultrasonic tactile feedback," in *2019 IEEE International Symposium on Multimedia (ISM)*, pp. 94–944, IEEE, 2019.

23. Carter, T., S. A. Seah, B. Long, B. Drinkwater, *et al.*, "Ultrahaptics: multi-point mid-air haptic feedback for touch surfaces," in *Proceedings of the 26th Annual ACM Symposium on User Interface Software and Technology*, pp. 505–514, 2013.

24. Frier, W., D. Pittera, D. Ablart, M. Obrist, *et al.*, "Sampling strategy for ultrasonic mid-air haptics," in *Proceedings of the 2019 CHI Conference on Human Factors in Computing Systems*, pp. 1–11, 2019.

25. Hajas, D., D. Pittera, A. Nasce, O. Georgiou, *et al.*, "Mid-air haptic rendering of 2d geometric shapes with a dynamic tactile pointer," *IEEE Transactions on Haptics*, Vol. 13, no. 4, pp. 806–817, 2020.

26. Nicci, "How does ultrahaptics technology work? - ultrahaptics developer information." Available at https://developer.old.ultrahaptics.com/knowledgebase/haptics-overview/, Jul 2018. Accessed: 2023-4-20.

27. Ultraleap, "How hand tracking works." Available at https://www.ultraleap.com/company/news/blog/how-hand-tracking-works/, Sep 2020. Accessed: 2023-4-22.

28. Burton, C., L. S. Chesterton, and G. Davenport, "Diagnosing and managing carpal tunnel syndrome in primary care," *British Journal of General Practice*, Vol. 64, no. 622, pp. 262–263, 2014.

29. "Nhs ayrshire arran-carpal tunnel syndrome." https://www.nhsaaa.net/allied-health-professionals-ahps/musculoskeletal- service/carpal-tunnel-syndrome. Accessed: 2023-4-22.

30. "Carpal tunnel syndrome fact sheet." https://aci.health.nsw.gov.au/netfactsheets/carpal-tunnel-syndrome. Accessed: 2023-4-20.

31. Żyluk, A., and I. Walaszek, "The effect of the involvement of the dominant or non-dominant hand on grip/pinch strengths and the levine score in patients with carpal tunnel syndrome," *Journal of Hand Surgery (European Volume)*, Vol. 37, no. 5, pp. 427–431, 2012.

32. Dyer, G., S. Lozano-Calderon, C. Gannon, M. Baratz, *et al.*, "Predictors of acute carpal tunnel syndrome associated with fracture of the distal radius," *The Journal of Hand Surgery*, Vol. 33, no. 8, pp. 1309–1313, 2008.

33. Osterman, M., A. M. Ilyas, and J. L. Matzon, "Carpal tunnel syndrome in pregnancy," *Orthopedic Clinics*, Vol. 43, no. 4, pp. 515–520, 2012.

34. Sawaya, R. A., and C. Sakr, "When is the phalen's test of diagnostic value: an electrophysiologic analysis?," *Journal of Clinical Neurophysiology*, Vol. 26, no. 2, pp. 132–133, 2009.

35. Graham, B., "The value added by electrodiagnostic testing in the diagnosis of carpal tunnel syndrome," *JBJS*, Vol. 90, no. 12, pp. 2587–2593, 2008.

36. Rosario, N. B., and O. De Jesus, "Electrodiagnostic evaluation of carpal tunnel syndrome," 2020.

37. Yoshii, Y., C. Zhao, and P. C. Amadio, "Recent advances in ultrasound diagnosis of carpal tunnel syndrome," *Diagnostics*, Vol. 10, no. 8, p. 596, 2020.

38. Jarvik, J. G., E. Yuen, and M. Kliot, "Diagnosis of carpal tunnel syndrome: electrodiagnostic and mr imaging evaluation," *Neuroimaging Clinics*, Vol. 14, no. 1, pp. 93–102, 2004.

39. Bland, J. D., "Carpal tunnel syndrome," *Current Opinion in Neurology*, Vol. 18, pp. 581–585, Oct 2005.

40. Wilder-Smith, E. P., R. C. Seet, and E. C. Lim, "Diagnosing carpal tunnel syndrome-clinical criteria and ancillary tests," *Nature Clinical Practice Neurology*, Vol. 2, no. 7, pp. 366–374, 2006.

41. "Harvard health, diagnosis of carpal tunnel syndrome: electrodiagnostic and mr imaging evaluation." https://www.health.harvard.edu/pain/taming-carpal-tunnel-syndrome, Jan 2013. Accessed: 2023-4-20.

42. Marshall, S. C., G. Tardif, and N. L. Ashworth, "Local corticosteroid injection for carpal tunnel syndrome," *Cochrane Database of Systematic Reviews*, no. 2, 2007.

43. Boyer, M. I., "Corticosteroid injection for carpal tunnel syndrome," *Journal of Hand Surgery*, Vol. 33, no. 8, pp. 1414–1416, 2008.

44. Piazzini, D. B., I. Aprile, P. E. Ferrara, C. Bertolini, *et al.*, "A systematic review of conservative treatment of carpal tunnel syndrome," *Clinical Rehabilitation*, Vol. 21, no. 4, pp. 299–314, 2007.

45. Lee, J.-J., S. M. Hwang, J. S. Jang, S. Y. Lim, *et al.*, "Remifentanil-propofol sedation as an ambulatory anesthesia for carpal tunnel release," *Journal of Korean Neurosurgical Society*, Vol. 48, no. 5, p. 429, 2010.

46. Al Youha, S., and D. H. Lalonde, "Update/review: changing of use of local anesthesia in the hand," *Plastic and Reconstructive Surgery Global Open*, Vol. 2, no. 5, 2014.

47. Nabhan, A., B. Ishak, J. Al-Khayat, and W.-I. Steudel, "Endoscopic carpal tunnel release using a modified application technique of local anesthesia: safety and effectiveness," *Journal of Brachial Plexus and Peripheral Nerve Injury*, Vol. 3, no. 01, pp. e35–e38, 2008.

48. Sherman, C., "The senses: The somatosensory system," *Dana Foundation*, Vol. 12, 2019.

49. Kandel, E. R., J. H. Schwartz, T. M. Jessell, S. A. Siegelbaum, and A. Hudspeth, "Principles of neural science, fifth editon," in *Principles of Neural Science*, McGraw-Hill Education, 2013.

50. Adibi, M., D. Zoccolan, and C. W. Clifford, "Sensory adaptation," 2021.

51. Roberts, D., "Signals and perception: The fundamentals of human sensation," *Palgrave Macmillan*, 2002.

52. Johnson, K. O., and S. S. Hsiao, "Neural mechanisms of tactual form and texture perception," *Annual Review of Neuroscience*, Vol. 15, no. 1, pp. 227–250, 1992.

53. Johnson, K. O., "The roles and functions of cutaneous mechanoreceptors," *Current Opinion in Neurobiology*, Vol. 11, no. 4, pp. 455–461, 2001.

54. Torebjörk, H. E., and J. L. Ochoa, "Specific sensations evoked by activity in single identified sensory units in man," *Acta Physiologica Scandinavica*, Vol. 110, no. 4, pp. 445–447, 1980.

55. Talbot, W. H., I. Darian-Smith, H. H. Kornhuber, and V. B. Mountcastle, "The sense of flutter-vibration: comparison of the human capacity with response patterns of mechanoreceptive afferents from the monkey hand.," *Journal of Neurophysiology*, Vol. 31, no. 2, pp. 301–334, 1968.

56. Pare, M., R. Elde, J. E. Mazurkiewicz, A. M. Smith, and F. L. Rice, "The meissner corpuscle revised: a multiafferented mechanoreceptor with nociceptor immunochemical properties," *Journal of Neuroscience*, Vol. 21, no. 18, pp. 7236–7246, 2001.

57. Biswas, A., M. Manivannan, and M. A. Srinivasan, "Multiscale layered biomechanical model of the pacinian corpuscle," *IEEE Transactions on Haptics*, Vol. 8, no. 1, pp. 31–42, 2014.

58. Biswas, A., M. Manivannan, and M. A. Srinivasan, "Vibrotactile sensitivity threshold: Nonlinear stochastic mechanotransduction model of the pacinian corpuscle," *IEEE Transactions on Haptics*, Vol. 8, no. 1, pp. 102–113, 2014.

59. Gescheider, G. A., "Evidence in support of the duplex theory of mechanoreception.," *Sensory Processes*, 1976.

60. Gescheider, G. A., B. F. Sklar, C. L. Van Doren, and R. T. Verrillo, "Vibrotactile forward masking: psychophysical evidence for a triplex theory of cutaneous mechanoreception," *The Journal of the Acoustical Society of America*, Vol. 78, no. 2, pp. 534–543, 1985.

61. Bolanowski Jr, S. J., G. A. Gescheider, R. T. Verrillo, and C. M. Checkosky, "Four channels mediate the mechanical aspects of touch," *The Journal of the Acoustical Society of America*, Vol. 84, no. 5, pp. 1680–1694, 1988.

62. Bolanowski Jr, S., and R. T. Verrillo, "Temperature and criterion effects in a somatosensory subsystem: a neurophysiological and psychophysical study.," *Journal of Neurophysiology*, Vol. 48, no. 3, pp. 836–855, 1982.

63. Capraro, A. J., R. T. Verrillo, and J. J. Zwislocki, "Psychophysical evidence for a triplex system of cutaneous mechanoreception.," *Sensory Processes*, 1979.

64. Gescheider, G. A., "Psychophysics: Method and theory.," 1976.

65. Gescheider, G. A., S. Bolanowski, K. Hall, K. Hoffman, and R. Verrillo, "The effects of aging on information-processing channels in the sense of touch: I. absolute sensitivity," *Somatosensory & Motor Research*, Vol. 11, no. 4, pp. 345–357, 1994.

66. Gescheider, G. A., S. J. Bolanowski, and R. T. Verrillo, "Some characteristics of tactile channels," *Behavioural Brain Research*, Vol. 148, no. 1-2, pp. 35–40, 2004.

67. Verrillo, R. T., "Temporal summation in vibrotactile sensitivity," *The Journal of the Acoustical Society of America*, Vol. 37, no. 5, pp. 843–846, 1965.

68. Gescheider, G. A., S. J. Bolanowski, J. V. Pope, and R. T. Verrillo, "A four-channel analysis of the tactile sensitivity of the fingertip: frequency selectivity, spatial summation, and temporal summation," *Somatosensory & Motor Research*, Vol. 19, no. 2, pp. 114–124, 2002.

69. Mohamad Hashim, I. H., S. Kumamoto, K. Takemura, T. Maeno, *et al.*, "Tactile evaluation feedback system for multi-layered structure inspired by human tactile perception mechanism," *Sensors*, Vol. 17, no. 11, p. 2601, 2017.

70. Buccino, G., F. Binkofski, G. R. Fink, L. Fadiga, *et al.*, "Action observation activates premotor and parietal areas in a somatotopic manner: an fmri study," in *Social Neuroscience*, pp. 133–141, Psychology Press, 2013.

71. Seelke, A. M., J. J. Padberg, E. Disbrow, S. M. Purnell, *et al.*, "Topographic maps within brodmann's area 5 of macaque monkeys," *Cerebral Cortex*, Vol. 22, no. 8, pp. 1834–1850, 2012.

72. "Touch central processing." https://openbooks.lib.msu.edu/neuroscience/chapter/touch-central-processing/. Accessed: 2023-4-20.

73. Geyer, S., A. Schleicher, and K. Zilles, "Areas 3a, 3b, and 1 of human primary somatosensory cortex: 1. microstructural organization and interindividual variability," *Neuroimage*, Vol. 10, no. 1, pp. 63–83, 1999.

74. Disbrow, E., E. Litinas, G. Recanzone, D. Slutsky, *et al.*, "Thalamocortical connections of the parietal ventral area (pv) and the second somatosensory area (s2) in macaque monkeys," *Thalamus & Related Systems*, Vol. 1, no. 4, pp. 289–302, 2002.

75. Kimura, J., "Electrodiagnosis in diseases of nerve and muscle: principles and practice," 2013.

76. Mallik, A., and A. Weir, "Nerve conduction studies: essentials and pitfalls in practice," *Journal of Neurology, Neurosurgery & Psychiatry*, Vol. 76, no. suppl 2, pp. ii23–ii31, 2005.

77. Urry, L. A., N. Meyers, M. L. Cain, S. A. Wasserman, *et al.*, *Campbell biology: Australian and New Zealand version*, Pearson Australia, 2021.

78. Jones, L. K., "Nerve conduction studies: basic concepts and patterns of abnormalities," *Neurologic Clinics*, Vol. 30, no. 2, pp. 405–427, 2012.

79. Sakly, G., Z. Affes, S. B. Dhia, A. Trabelsi, *et al.*, "The impact of carpal tunnel syndrome on ulnar nerve: an electro-clinical study," *J Neurol Neurosci*, Vol. 7, no. 5, 2016.

80. Novello, B. J., and T. Pobre, "Electrodiagnostic evaluation of peripheral neuropathy," 2020.

81. Shanina, E., and R. G. Smith, "Electrodiagnostic evaluation of myopathy," 2020.

82. Tamarkin, R. G., and A. C. Isaacson, "Electrodiagnostic evaluation of lumbosacral radiculopathy," in *StatPearls [Internet]*, StatPearls Publishing, 2022.

83. Güçlü, B., and Ç. Öztek, "Tactile sensitivity of children: effects of frequency, masking, and the non-pacinian i psychophysical channel," *Journal of Experimental Child Psychology*, Vol. 98, no. 2, pp. 113–130, 2007.

84. Zwislocki, J. J., and E. M. Relkin, "On a psychophysical transformed-rule up and down method converging on a 75% level of correct responses," *Proceedings of the National Academy of Sciences*, Vol. 98, no. 8, pp. 4811–4814, 2001.

85. Brooke, J., *et al.*, "Sus-a quick and dirty usability scale," *Usability Evaluation in Industry*, Vol. 189, no. 194, pp. 4–7, 1996.

86. Multanen, J., J. Ylinen, T. Karjalainen, J. Ikonen, *et al.*, "Structural validity of the boston carpal tunnel questionnaire and its short version, the 6-item cts symptoms scale: a rasch analysis one year after surgery," *BMC Musculoskeletal Disorders*, Vol. 21, pp. 1–14, 2020.

87. "American academy of orthopaedic surgeons - carpal tunnel syndrome exercise program." Available at https://orthoinfo.aaos.org/en/recovery/carpal-tunnel-syndrome-therapeutic-exercise-program/. Accessed: 2023-4-20.

88. "Preparing assets for unity-scale and unit." https://docs.unity3d.com/2019.3/Documentation/Manual/BestPracticeMakingBelievableVisuals1.html. Accessed: 2023-5-15.

89. Jensen, M. P., C. Chen, and A. M. Brugger, "Interpretation of visual analog scale ratings and change scores: a reanalysis of two clinical trials of postoperative pain," *The Journal of Pain*, Vol. 4, no. 7, pp. 407–414, 2003.

90. Sarilar, A. C., D. K. Gök, *et al.*, "Value of boston questionnaire in carpal tunnel syndrome," *Neurological Sciences and Neurophysiology*, Vol. 38, no. 4, p. 245, 2021.

91. Sasaki, T., T. Koyama, T. Kuroiwa, A. Nimura, *et al.*, "Evaluation of the existing electrophysiological severity classifications in carpal tunnel syndrome," *Journal of Clinical Medicine*, Vol. 11, no. 6, p. 1685, 2022.

92. Bland, J. D., "A neurophysiological grading scale for carpal tunnel syndrome," *Muscle & Nerve: Official Journal of the American Association of Electrodiagnostic Medicine*, Vol. 23, no. 8, pp. 1280–1283, 2000.

93. Elnady, B., E. M. Rageh, T. Ekhouly, S. M. Fathy, *et al.*, "Diagnostic potential of ultrasound in carpal tunnel syndrome with different etiologies: correlation of sonographic median nerve measures with electrodiagnostic severity," Vol. 20, pp. 1–8, 2019.

94. Georgiev, G. P., V. Karabinov, G. Kotov, and A. Iliev, "Medical ultrasound in the evaluation of the carpal tunnel: a critical review," *Cureus*, Vol. 10, no. 10, 2018.

95. Wiesler, E. R., G. D. Chloros, M. S. Cartwright, B. P. Smith, *et al.*, "The use of diagnostic ultrasound in carpal tunnel syndrome," *The Journal of Hand Surgery*, Vol. 31, no. 5, pp. 726–732, 2006.

96. Balint, P., and K. Althoefer, "Medical virtual reality palpation training using ultrasound based haptics and image processing," *Proc. Jt. Work. New Technol. Comput. Assist. Surg*, 2018.

97. Paneva, V., S. Seinfeld, M. Kraiczi, and J. Müller, "Haptiread: Reading braille as mid-air haptic information," in *Proceedings of the 2020 ACM Designing Interactive Systems Conference*, pp. 13–20, 2020.

98. Cho, H., and K.-Y. Sohng, "The effect of a virtual reality exercise program on physical fitness, body composition, and fatigue in hemodialysis patients," *Journal of Physical Therapy Science*, Vol. 26, no. 10, pp. 1661–1665, 2014.

99. Finkelstein, S., T. Barnes, Z. Wartell, and E. A. Suma, "Evaluation of the exertion and motivation factors of a virtual reality exercise game for children with autism," in *2013 1st Workshop on Virtual and Augmented Assistive Technology (VAAT)*, pp. 11–16, IEEE, 2013.

100. Park, E.-C., S.-G. Kim, and C.-W. Lee, "The effects of virtual reality game exercise on balance and gait of the elderly," *Journal of Physical Therapy Science*, Vol. 27, no. 4, pp. 1157–1159, 2015.

101. Zeng, N., Z. Pope, and Z. Gao, "Acute effect of virtual reality exercise bike games on college students' physiological and psychological outcomes," *Cyberpsychology, Behavior, and Social Networking*, Vol. 20, no. 7, pp. 453–457, 2017.

102. Mulot, L., T. Howard, C. Pacchierotti, and M. Marchal, "Ultrasound mid-air haptics for hand guidance in virtual reality," *IEEE Transactions on Haptics*, 2023.

103. Vaquero-Melchor, D., and A. M. Bernardos, "Enhancing interaction with augmented reality through mid-air haptic feedback: Architecture design and user feedback," *Applied Sciences*, Vol. 9, no. 23, p. 5123, 2019.

104. Smith, J. L., and N. A. Ebraheim, "Anatomy of the palmar cutaneous branch of the median nerve: a review," *Journal of Orthopaedics*, Vol. 16, no. 6, pp. 576–579, 2019.

105. Uluc, K., I. Aktas, G. Sunter, P. Kahraman Koytak, *et al.*, "Palmar cutaneous nerve conduction in patients with carpal tunnel syndrome," *International Journal of Neuroscience*, Vol. 125, no. 11, pp. 817–822, 2015.

106. Rathakrishnan, R., A. K. Therimadasamy, Y. Chan, and E. Wilder-Smith, "The median palmar cutaneous nerve in normal subjects and cts," *Clinical Neurophysiology*, Vol. 118, no. 4, pp. 776–780, 2007.

107. Godlewski, B., R. Czepko, T. Gierula, and G. Klauz, "Anatomic aspects of the carpal tunnel release surgery," *Austin Journal of Neurosurgery*, Vol. 1, p. 4, 01 2014.

108. Dhong, E. S., S. K. Han, B. Lee, and W. K. Kim, "Correlation of electrodiagnostic findings with subjective symptoms in carpal tunnel syndrome.," *Annals of Plastic Surgery*, Vol. 45, no. 2, pp. 127–131, 2000.

109. Yang, A., P. Cavanaugh, P. K. Beredjiklian, J. L. Matzon, *et al.*, "Correlation of carpal tunnel syndrome 6 score and physical exam maneuvers with electrodiagnostic test severity in carpal tunnel syndrome: A blinded prospective cohort study," *The Journal of Hand Surgery*, Vol. 48, no. 4, pp. 335–339, 2023.

110. Hoshi, T., M. Takahashi, T. Iwamoto, and H. Shinoda, "Noncontact tactile display based on radiation pressure of airborne ultrasound," *IEEE Transactions on Haptics*, Vol. 3, no. 3, pp. 155–165, 2010.

111. Ito, M., D. Wakuda, Y. Makino, and H. Shinoda, "Hybrid focus using 70 and 40 khz ultrasound in mid-air tactile display," in *Haptic Interaction: Science, Engineering and Design 2*, pp. 131–134, Springer, 2018.